Załącznik nr 3 w postępowaniu habilitacyjnym – Autoreferat w wersji angielskiej

Summary of professional achievements

Bartłomiej Wiendlocha

AGH University of Science and Technology
Faculty of Physics and Applied Computer Science

Krakow, June 4, 2018

Contents

1. Personal data

Name and surname: Bartłomiej Wiendlocha
Current employment: AGH University of Science and Technology
Faculty of Physics and Applied Computer Science
Department of Condensed Matter Physics
Phone: +48 12 617 29 55
e-mail: wiendlocha@fis.agh.edu.pl

2. Diplomas and scientific degrees

1. **Master of Science in technical physics**, 14.06.2004. AGH University of Science and Technology, Faculty of Physics and Applied Computer Science. Master thesis title: *Calculations of the electron-phonon properties of MgB_2 and $MgCNi_3$-type superconductors*, thesis supervisor dr hab. Janusz Toboła. Diploma with honors.

2. **Ph. D. in physics**, 25.05.2009. AGH University of Science and Technology, Faculty of Physics and Applied Computer Science. Ph. D. thesis title: *Theoretical studies of the superconducting and magnetic properties of the selected intermetallic compounds*, thesis supervisor dr hab. Janusz Toboła. Diploma with honors.

3. Employment in scientific institutions

1. 10.2008 – 09.2010, assistant at the Faculty of Physics and Applied Computer Science, AGH University of Science and Technology in Krakow, Poland

2. 10.2010 – until now, assistant professor at the Faculty of Physics and Applied Computer Science, AGH University of Science and Technology in Krakow, Poland

3. 03.2011 – 08.2011, Postdoctoral researcher, Department of Mechanical and Aerospace Engineering, the Ohio State University, Columbus, Ohio, USA.

4. 07.2012 – 08.2012, Postdoctoral researcher, Department of Mechanical and Aerospace Engineering, the Ohio State University, Columbus, Ohio, USA.

5. 03.2014 – 08.2014, Postdoctoral researcher, Department of Mechanical and Aerospace Engineering, the Ohio State University, Columbus, Ohio, USA.

4. Scientific achievement, following the law on scientific degrees

As a scientific achievement, being the base of the current application, I present a series of articles on a common topic.

4.1. Title of the achievement

Resonant impurities in the thermoelectric materials – electronic structure and transport properties.

4.2. Authors, titles of publications, publication year, publisher

[**H1**] C. M. Jaworski, **B. Wiendlocha**, V. Jovovic and J. P. Heremans, "Combining alloy scattering of phonons and resonant electronic levels to reach a high thermoelectric figure of merit in PbTeSe and PbTeS alloys" Energy & Environmental Science **4**, 4155 (2011). [IF 9.6]

[**H2**] C.M. Orovets, A.M. Chamoire, H. Jin, **B. Wiendlocha** and J.P. Heremans, "Lithium as an Interstitial Donor in Bismuth and Bismuth-Antimony Alloys", Journal of Electronic Materials **41**, 1648 (2012). [IF 1.6]

[**H3**] J. P. Heremans, **B. Wiendlocha** and A. M. Chamoire "Resonant levels in bulk thermoelectric semiconductors" Energy & Environmental Science **5**, 5510 (2012). [IF 11.6]

[**H4**] **B. Wiendlocha**, "Fermi surface and electron dispersion of PbTe doped with resonant Tl impurity from KKR-CPA calculations", Physical Review B **88**, 205205 (2013). [IF 3.7]

[**H5**] **B. Wiendlocha**, "Localization and magnetism of the resonant impurity states in Ti doped PbTe", Applied Physics Letters **105**, 133901 (2014). [IF 3.3]

[**H6**] S. Kim, **B. Wiendlocha**, H. Jin, J. Tobola, J.P. Heremans, "Electronic structure and thermoelectric properties of p-type Ag-doped Mg_2Sn and $Mg_2Sn_{1-x}Si_x$ ($x = 0.05, 0.1$)", Journal of Applied Physics **116**, 153706 (2014). [IF 2.2]

[**H7**] H. Jin, **B. Wiendlocha** and J. P. Heremans, "P-type doping of elemental bismuth with indium, gallium and tin: a novel doping mechanism in solids" Energy & Environmental Science **8**, 2027 (2015). [IF 25.4]

[**H8**] **B. Wiendlocha**, K. Kutorasiński, S. Kaprzyk, J. Tobola, "Recent progress in calculations of electronic and transport properties of disordered thermoelectric materials", Scripta Materialia **111**, 33 (2016). [IF 3.7]

[**H9**] **B. Wiendlocha**, "Resonant Levels, Vacancies, and Doping in Bi_2Te_3, Bi_2Te_2Se, and Bi_2Se_3 Tetradymites", Journal of Electronic Materials **45**, 3515 (2016). [IF 1.6]

[**H10**] J.P. Heremans, **B. Wiendlocha**, H. Jin, Thermoelectric Materials with Resonant States, rozdział rozdział 11.3 (strony 441 - 451) w monografii *Advanced Thermoelectrics: Materials, Contacts, Devices, and Systems*, ed. Z. Ren, Y. Lan, Qi. Zhang, CRC Press, Taylor & Francis Group, Boca Raton, FL (USA), 2018.

[**H11**] **B. Wiendlocha**, J-B. Vaney, C. Candolfi, A. Dauscher, B. Lenoir, and J. Tobola, "An Sn-induced resonant level in β-As_2Te_3", Physical Chemistry Chemical Physics **20**, 12948 (2018). [IF* 4.1]

[**H12**] **B. Wiendlocha**, "Thermopower of thermoelectric materials with resonant levels: PbTe:Tl versus PbTe:Na and $Cu_{1-x}Ni_x$", Physical Review B **97**, 205203 (2018). [IF* 3.8]

The values of Impact Factor (IF) coefficients are given after the Journal Citation Reports base, according to the year of publication or (*) with the latest available value.

The co-authors' statements regarding their contribution to the above -mentioned publications can be found in **attachment no 5**: *co-authors' statements.*

4.3. Description of the aim of the articles listed above and the results obtained as well as their possible application

Introduction

The subject matter I have dealt with in recent years and which is the subject of this habilitation focuses on thermoelectric materials, thus it is a combination of basic scientific research in the field of quantum mechanics and solid state theory with extremely important possibilities of applying research results in technology and everyday life. bf Thermoelectric (TE) materials are materials in which it is possible to directly convert thermal energy into electricity, which is possible due to the occurrence of *the Seebeck effect* [1]. It consists in inducing in the material the gradient of the electrical potential through a temperature gradient. If we build a circuit by connecting two different TE materials, and the two contact points will have different temperature, the current will flow. As a result opposite to the Seebeck effect, namely in the effect of Peltier, [1], it is possible to cool one contact point thanks to the flow of electric current through the module. Thus, using thermoelectric materials, it is possible to build energy conversion devices. Thermoelectric generators, using the temperature difference to generate electric voltage, and thermoelectric coolers, in which thanks to the current flow cooling of one of the parts of the system takes place, they are devices that do not contain moving elements, and thanks to this reliable and practically maintenance-free. These features determined the use of TE generators in space applications [2] - thermoelectrics are present in the space exploration from the 1950s, including vehicles moving on the surface of Mars (for example, Mars Rover Curiosity, exploring the surface of Mars since 2011). In addition, the ever-growing global demand for electricity and the need to reduce CO_2 have resulted in a significant increase in interest in TE materials in the last decade. For example, TE generators, recovering some of the energy lost in the combustion of fuel in cars, are to contribute to fuel economy and reduction of carbon dioxide emissions. Such generators are already assembled in test cars by leading automotive concerns [3]. Cooling with thermoelectric effects, in addition to obvious applications, e.g. in commercially available portable thermoelectric refrigerators (in particular the automotive ones), can be used to obtain cryogenic temperatures (less than 100 kelvins), where conventional cooling requires the use of coolers of considerable size and weight. Due to this, the possibility of using TE coolers in X, gamma and infrared detectors in military drones and satellites was examined, where the weight of an element plays a key role. The issue of searching for efficient materials for this purpose was the subject of the project *Cryogenic Peltier Cooling* funded by the US Air Force Office of Scientific Research, in which I was involved while staying at Ohio State University (OSU) in the United States, between 2011 and 2014.

The constant challenge and the proverbial "Achilles' heel" of TE systems is their efficiency, reaching at most a dozen or so percent, being still lower, than obtained in traditional gas-based generators, or refrigerators, based on gas expansion cycle. This limits the use of thermoelectrics on a wider scale. The key to improving the efficiency of TE elements is to find the material with the highest so-called

figure-of-merit zT [1], defined as:

$$zT = \frac{S^2\sigma}{\kappa}T \tag{1}$$

where S is a thermopower (also known as the Seebeck coefficient), σ is the electrical conductivity, κ is the thermal conductivity, and T is the absolute temperature. Currently, typically used materials have $zT \sim 1.0$, it is desirable to raise zT to the level of $2.0 - 3.0$ in the widest range of temperatures. Currently, the record value of $zT = 2.6$ was found in the semiconductor SnSe [4], along one of the crystallographic directions, at a temperature of over 900 K. Unfortunately due to the existence of a phase transition around 800 K, accompanied by a sudden change in volume, the problem may be to use it in a practical devices in the vicinity of this temperature.

Thermopower S is directly related to the energy-dependent electrical conductivity (so-called transport function) $\sigma(E)$:

$$\sigma(E) = e^2 \sum_n \int \frac{d\mathbf{k}}{4\pi^3} \tau_n(\mathbf{k}) \mathbf{v}_n(\mathbf{k}) \otimes \mathbf{v}_n(\mathbf{k}) \delta(E - E_n(\mathbf{k})). \tag{2}$$

where e is the elementary charge, τ is the carriers' scattering time, and $\mathbf{v}$ is their velocity. Integrals of the transport function give the electric conductivity σ and the thermopower S:

$$\sigma_e = L^{(0)}, \quad S = -\frac{1}{eT}\frac{L^{(1)}}{L^{(0)}}, \tag{3}$$

where

$$L^{(\alpha)} = \int dE \left(-\frac{\partial f}{\partial E}\right) (E - \mu_c)^\alpha \sigma(E). \tag{4}$$

The value of the chemical potential μ_c depends on the temperature and carrier concentration, and is independently determined in every step of the calculation.

The problem of increasing the value of zT is so difficult because the values defining this coefficient have opposite tendencies, i.e. the material exhibiting high electrical conductivity usually has a very low Seebeck coefficient, which gives a low value of the product $S^2\sigma$ (power factor), and additionally high electrical conductivity entails high electron thermal conductivity κ_e, which raises the value of κ, resulting in a low value of the quotient $S^2\sigma/\kappa$.

Therefore, the best TE materials at present are properly doped semiconductors with a narrow band gap, where the key to developing an efficient TE material is the right choice of material and optimization of charge carrier concentration, ensuring the right balance between electrical, thermal and heat conductivity. In a typical TE semiconductor material, the role of doping atoms is only to introduce free charge carriers into the base material – electrons (donor dopants) or holes (acceptor dopants) – while the transport properties of the system is mainly determined by the electronic structure of the host material. This is because in most cases, substitution of a small number of the host atoms with dopant atoms does not cause significant changes in the electronic structure of the system, except for the shift of the Fermi level by the electrically active dopants. This allows the control of the charge concentration and in particular leaving the semiconductor state to increase the electrical conductivity.

But this is not the only possibility of the dopant atoms' action in thermoelectrics. As demonstrated by the team of Joseph Heremans in experimental work in 2008, [5] on the example of the well-known PbTe semiconductor doped with thallium (Tl), the modification and improvement of thermoelectric properties can be obtained if we can introduce a *resonant impurity*, which forms the so-called bf resonant level (RL). Such resonant impurity does not only modify the carrier concentration (Tl is an acceptor in PbTe), but also strongly modifies the electronic structure of the doped compound, forming the resonant state.

Resonant energy levels may be formed by dopant atoms added to metals or semiconductors, at energy, at which in the absence of neighboring atoms a bound state would be formed [6, 7, 8]. For semiconductors, this energy may be inside the valence or conduction bands, and than such a resonant level (RL) strongly distorts the electronic band structure of the host material, violating the rigid-band doping model. The problem of impurity-induced resonant levels has been known in solid state physics since 1950., from the early works on diluted metallic alloys (see, e.g. works of Korringa [9, 10] or Friedel [11], literature on RLs in semiconductors is reviewed in Ref. [7]). The best method for detecting the resonant state is to perform calculations of the electronic structure for a very small concentration of dopant atoms (in the order of 0.1%). Then we observe the formation of a very narrow peak in the partial density of electron states on dopant atoms', which will then evolve in different ways (depending on the dopant and doped material) for higher level of doping.

Through the resonant state, Tl introduced into PbTe causes the increase of the density of electronic states near the edge of the valence band, which was interpreted as the reason for a significant increase in the thermopower of the material (from about 55 μV/K to 125 μV/K at T = 300 K for the concentration of holes $p = 5 \cdot 10^{19}$ cm^{-3}), without drastically reducing electrical conductivity at high temperatures. Thanks to this, a high value of $zT = 1.5$ was obtained in T = 773 K in PbTe, much higher than obtained these days in this material using other doping. The possibility of formation of resonant states on dopant atoms in metals or semiconductors was a fact known earlier, however, mainly doping effects caused by the transition metals, with significantly different properties, have been studied, and no thorough research has been carried out regarding thermoelectric properties, in particular at room temperatures and above. The resonant states created on transition metals in alloys with noble metal

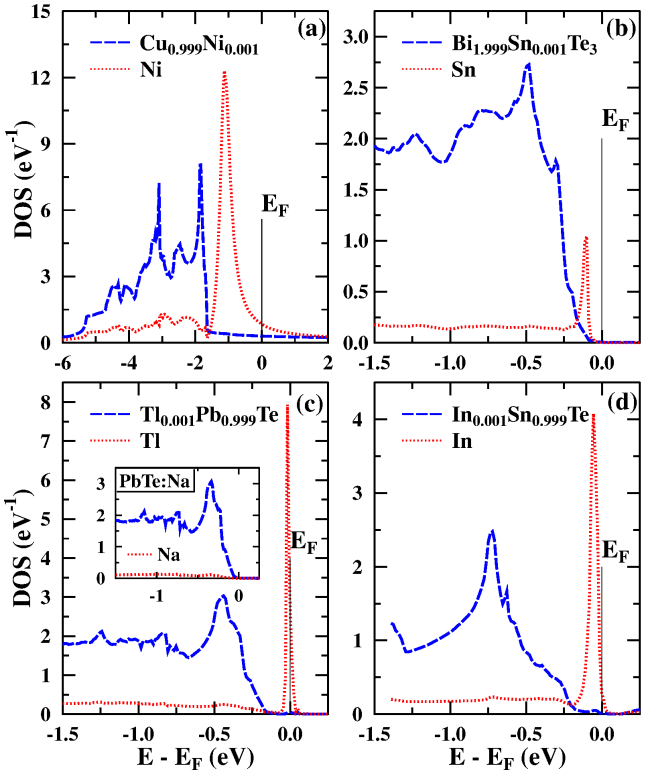

Figure 1: Formation of the resonant states on impurity atoms in Cu:Ni, Bi_2Te_3:Sn, PbTe:Tl and SnTe:In, shown by formation of a narrow DOS peak for small impurity concentrations. Inset in panel (c) shows the example of a "regular" dopant Na in PbTe. Figure from publication [**H8**].

(eg Cu-Ni or Ag-Pd) were much better known earlier. The results and idea published in [5] have received wide echoes in the thermoelectric community ([5] has currently about 2,000 citations) and caused a lot of interest in the subject of resonant states. The search for resonant impurities with similar properties in other materials has also begun, with at least several successes. However, the lack of a solid theoretical explanation of the influence of resonant dopants on the electronic structure and transport properties caused that some researchers remained skeptical about the idea of "resonant" improvement of thermoelectric properties, and indirectly initiated my work in this field.

The subject of thermoelectric materials and resonant impurities I began to deal with during a postdoctoral contract in the above-mentioned group of prof. Joseph Heremans at the State University of Columbus, Ohio in 2011 as part of the project it Cryogenic Peltier Cooling. It was a new topic for me, because earlier I was dealing mainly with research on the electronic structure of superconductors and magnetic materials, which was also the subject of my Ph. D. thesis, finished in 2009. I did not abandon the subject of superconductors, and I continued this research in parallel to work on thermoelectrics. In the period from Ph.D. defense to the present I was the author or co-author of 28 scientific publications, of which 9 concerned superconductors and 18 thermoelectric materials. 12 works, **[H1]** – **[H12]**, deal with resonant states and were chosen by me as a set of monothematic publications, which is the basis for applying for the habilitation degree.

Methods

My research work is based mainly on theoretical calculations of the electronic structure and related properties, for crystalline materials. The calculations are made within the framework of the DFT - it Density Functional Theory [12], using various complementary methods. In particular, in the works included in the habilitation achievement, the methods of KKR (Korringa-Kohn-Rostoker) and KKR-CPA (KKR with coherent potential approximation, CPA) and the method of linearized augmented plane waves (LAPW). These methods are implemented in several numerical codes, which I used, namely the family of KKR-CPA codes by Prof. Stanisław Kaprzyk from the Department of Condensed Matter Physics at WFiIS AGH [13, 14, 15], SPRKKR code [16, 17], developed in the group of Prof. Hubert Ebert from Ludwig-Maximilians-Universität München, and WIEN2K code [18] written in the group of Prof. Peter Blaha and Prof. Karlheinz Schwartz from Technische Universität Wien.

Research aim

In my work on resonant impurities, four basic goals can be distinguished:

- To examine the general influence of selected dopants on the electronic structure of a given material and determine if they form resonant states (all the papers, **[H1]**–**[H12]**)
- To examine, whether the resonant impurities form separated impurity bands and whether they tend to localize (papers **[H4]**, **[H5]**, **[H6]**, **[H8]**)
- Search for new resonant impurities (papers **[H2]**, **[H6]**, **[H7]**, **[H9]** , **[H10]**, **[H11]**)
- To confirm, basing on the theoretical calculations, the increase of thermopower due to presence of the resonant level and explaining the mechanism of increase (papers **[H3]**, **[H4]**, **[H5]** and especially **[H12]**);

In cooperation with the experimental group from the Ohio State University, six of these works were done, work **[H11]** was done in collaboration with an experimental group from Nancy (France), the rest are theoretical-only works, in 4 of which I am the only author.

In the following part of this self-review, I will discuss the most important results of the selected works, in chronological order, along with the context that accompanied them. Generally speaking, my contribution to all of the mentioned publications was performing the calculations of the electronic structure of the studied systems, analyzing them in terms of forming of the resonant states and their influence on the electronic properties, and analyzing the experimental results in the context of the obtained theoretical results.

Overview of the publications

[**H1**] C. M. Jaworski, B. Wiendlocha, V. Jovovic and J. P. Heremans, "Combining alloy scattering of phonons and resonant electronic levels to reach a high thermoelectric figure of merit in PbTeSe and PbTeS alloys" Energy & Environmental Science **4**, 4155 (2011).

After finding the increase of the thermopower and the improvement of thermoelectric efficiency in PbTe, under the influence of Tl resonant level in [5], a natural question arose whether further optimization of the TE properties is possible, eg. by lowering the thermal conductivity κ of the material. In the paper [**H1**] the properties of Pb(Te-Se) and Pb(Te-S) alloys doped with Tl were analyzed, in order to check whether the resonant state "survives" in the PbTe alloy with sulfur and selenium, and whether the resonance effect can be combined with the alloy scattering of phonons, induced by the Te/S and Te/Se substitution , to reduce the thermal conductivity κ, and boost zT values. The experimental results showed a rather surprising and initially unclear effect that the Seebeck coefficients of PbTeS and PbTeSe alloys doped with 2% of Tl practically does not change, reaching values similar to those in the "clean" PbTe after doping with Tl. Even at about 10% substitutions of Te, although different samples showed differences in carrier concentrations as large as an order of magnitude ($10^{19} - 10^{20}$ cm^{-3}), the thermopower remained in around 120μV/K at $T = 300$ K, which was of course a very desirable result (see Figure 2).

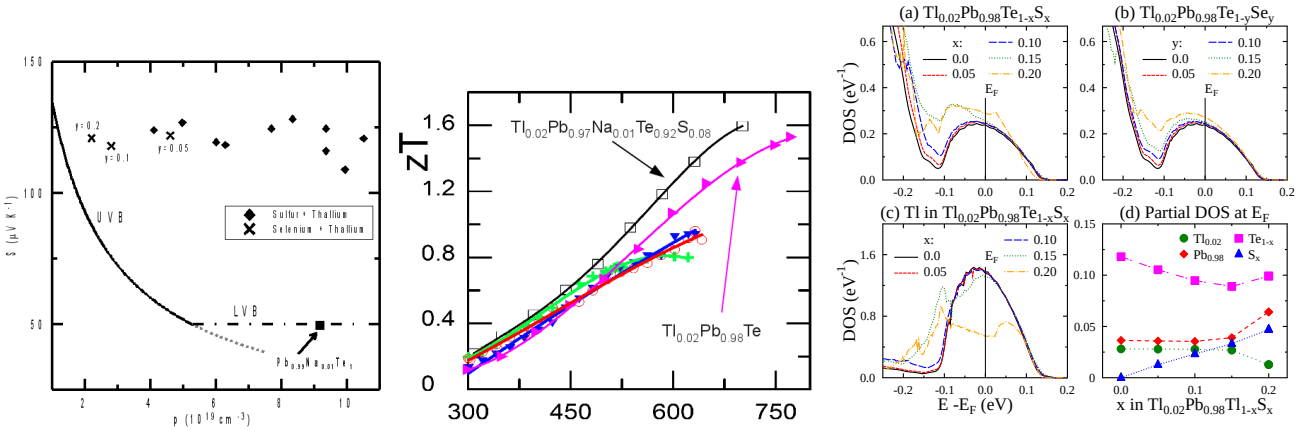

Figure 2: On the left: Pisarenko curve (thermopower as a function of carrier concentration) for PbTe, PbTeS:Tl and PbTeSe:Tl. The resonantly increased thermopower is maintained in a wide range of carrier concentrations and after the substitution of Te/Se and Te/S, in particular for the range of higher concentrations of p. The solid lines and the dash-dot line define the reference level of the PbTe thermopower doped with "non-resonant" impurities (eg with Na); UVB means upper valence band, LVB - lower valence band. In the middle: zT as the function of temperature, visible increase through the combination of the resonance and alloy scattering. On the right: resonant "hump" in the electronic density of states near the edge of the valence band in the studied materials, as a function of the concentration of Se and S. It can be seen that the resonant state persists without significant changes to about 15% substitution.

At the same time, due to the presence of chemical disorder (Te-Se, Te-S substitution), the effects of phonon scattering have been increased, resulting in a decrease in the thermal conductivity. The best results were obtained for the substitution of Te/S to about 10% concentration of S, for larger concentrations the efficiency of resonance in improving the TE properties seemed to worsen. In order to increase the concentration of carriers and electrical conductivity in the optimal sample, an additional 1% Na was added, which only slightly decreased the thermopower, but allowed to raise the power factor. Overall, thanks to the presence of resonance effect and phonon scattering, we managed to raise the zT to about 1.6 in T = 700 K, improving zT in a wide temperature range, compared to PbTe:Tl, which can be seen in Fig. 2.

In order to theoretically examine the evolution of the electronic structure of the system, and in particular to explain why the obtained thermopower is insensitive to the presence of Te/S and Te/Se substitutions, and constant in a wide range of charge concentration, I performed the KKR-CPA calculation for PbTe, $Tl_{0.02}PbTe_{1-x}S_x$ and $Tl_{0.02}PbTe_{1-y}Se_y$ in the concentration range $x, y \in (0.00, 0.20)$.

The analysis of the calculated density of electronic states $n(E)$ confirmed above all that the resonance state, whose source are Tl atoms, is also formed in the PbTeS and PbTeSe alloys, and the shape of the state density function itself does not change significantly upon the Te/S and Te/Se substitutions to around a dozen or so percent. In addition, despite the "resonant" state density at the Fermi level, the $n(E)$ curve, from the band edge to the E_F area, can be quite well described by the elemental $\propto \sqrt{E}$ dependence, characteristic of free electron model (see Fig. S4 in the supplementary material of the publication), with a constant value of the effective mass $m_D^* \simeq 1.5$, close to the experimentally deducted (1.35). Because for a single-band material $S \propto m_D^*$, this justifies the experimentally observed effect of a constant thermopower in a wide range of carrier concentration in PbTeS:Tl and PbTeSe:Tl, and maintaining a high value of S (because m_D^* in PbTe without resonance is lower) in the presence of substitutions at Te site. At about 20% of the Te/S or Te/Se substitution the density of states function in alloys began to change. It was shown that this was not related to the mere replacement of the Te atoms with sulfur or selenium, but was the effect of a negative chemical pressure – the lattice constant decreases upon the Te/S and Te/Se substitutions and this causes the resonant state to begin to "dissolve". The above observations allowed to formulate some important, qualitative conclusions:

- The free-electron-like shape of the density of states function $n(E)$ suggests strongly delocalized character of the resonant electronic states.

- Based on the analysis of the character of the single-particle wave functions, the Tl atom, although it is a resonance source, gives a small contribution to the density of states in the resonant $n(E)$ (a dozen or so percent), and most of the contribution comes from the Pb and Te electrons (host). Thus, the resonance effect is to a greater extent based on the disruption of the original Bloch's electron states of the PbTe crystal, than on the introduction of new localized states from the dopant atoms.

- In order for the resonance effect to be beneficial for the thermoelectric material, it is necessary to ensure a proper balance between the location and the delocalization of the electronic states around the dopant atoms. Too large delocalization of dopant states, induced here by chemical pressure, causes a "blurring" of the resonance and a lost in its efficiency. In turn, the too large location of the electron states could give a sharp maximum of the density of electron states (and high value of thermopower), but at the same time could lead to too small electrical conductivity, excluding material from applications.

In subsequent works, these conclusions will be further supported by more extended theoretical calculations.

[**H2**] C.M. Orovets, A.M. Chamoire, H. Jin, B. Wiendlocha, J.P. Heremans, "Lithium as an Interstitial Donor in Bismuth and Bismuth-Antimony Alloys", Journal of Electronic Materials **41**, 1648 (2012).

This work was part of the already mentioned project it Cryogenic Peltier Cooling searching for resonant impurities for semi-metallic bismuth (Bi) and semiconducting bismuth-antimony alloy (Bi-Sb), due to very good thermoelectric properties of Bi-Sb at low temperatures. In this work, the electron and thermoelectric properties of the above-mentioned systems after doping with lithium atoms (Li) were studied. Calculations of the electronic structure have shown that the lithium atom can lead to the formation of the resonant state in Bi and Bi-Sb, because a narrow peak in the density of electronic states on Li is formed, which is characteristic of the resonant state. Such a situation will only take place when the Li atoms are occupying the crystallographic positions of Bi (Sb) in the unit cell. In a case

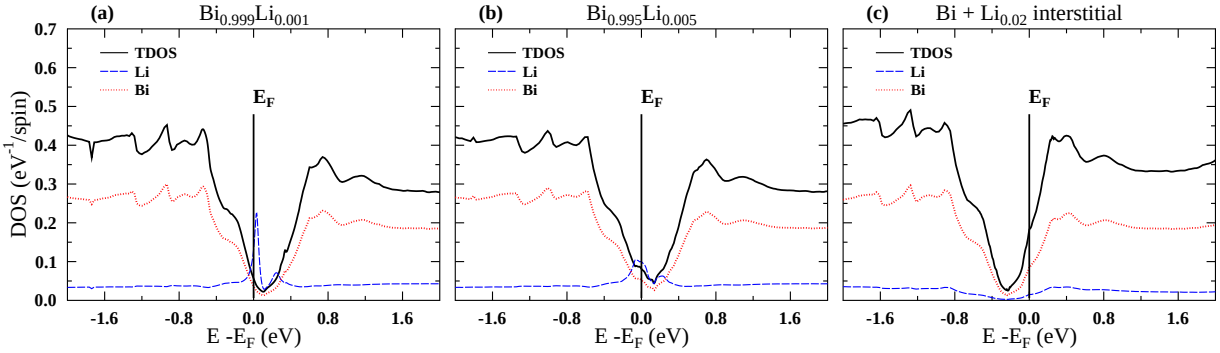

Figure 3: Calculated density of states for lithium-doped bismuth, (a-b) for the case where Li substitutes Bi, a resonant state is possible; (c) for the case where Li is located in the interstitial position, it behaves like a one-electron donor, only shifting the Fermi level.

when Li atoms were located in interstitial sites, Li was predicted to behave like a regular one-electron donor. Transport measurements carried out on the synthesized Bi:Li and Bi-Sb:Li samples showed that the systems behave as typical n-type doped Bi/Bi-Sb, which is consistent with the calculations for the interstitial location of Li in Bi and Bi-Sb. This allowed to classify Li as an interstitial donor in Bi and Bi-Sb alloy.

[**H3**] J. P. Heremans, B. Wiendlocha and A. M. Chamoire "Resonant levels in bulk thermoelectric semiconductors" Energy & Environmental Science **5**, 5510 (2012).

This publication is in part a review paper, discussing experimentally observed (at that time) resonant states in semiconductors. However, apart from the review part, it contains an original and earlier unpublished theoretical model of the impact of the resonance state on the thermopower, which I prepared for the purposes of this article.

The work presents, for the first time, with the help of a simplified theoretical model, how the increase in the density of states through the resonant state can lead to an increase in the thermopower (details in the publication). It was shown above all that the peak in the density of electron states can lead to a boost in S, as illustrated in Fig. 4. Raising S by the increase in DOS is possible at both low and high temperatures, while the so-called resonant scattering, which previous studies on

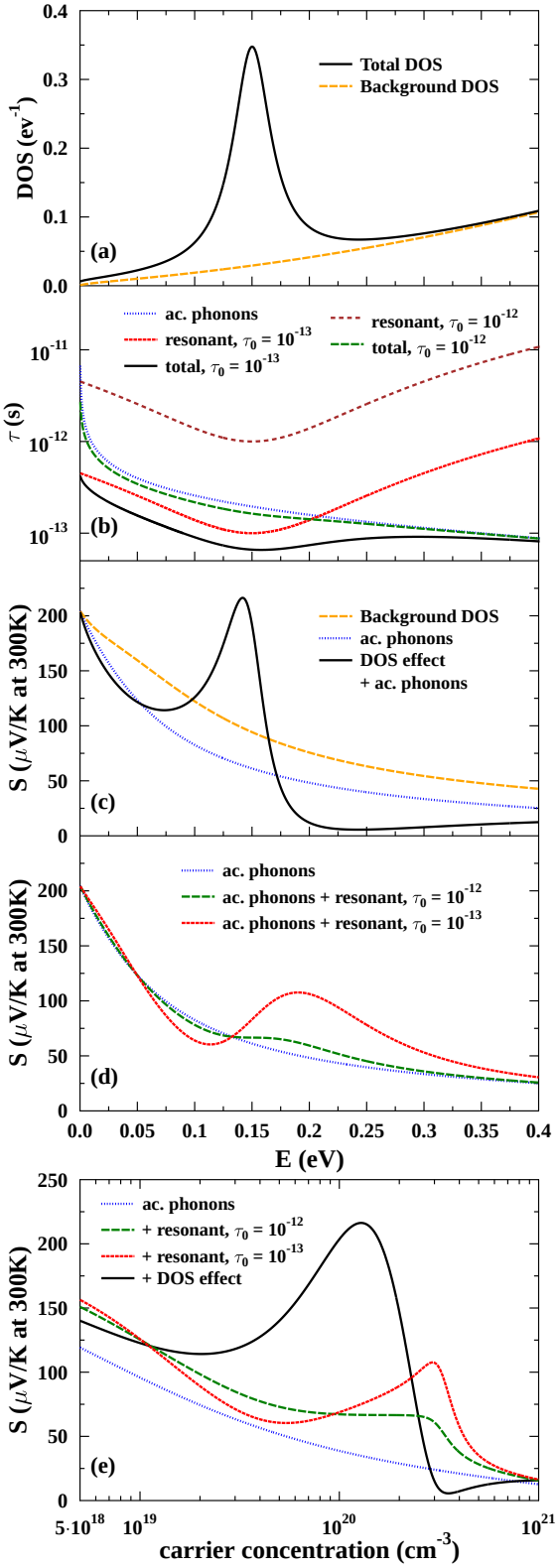

Figure 4: Schematic representation of the effect of a density of states (DOS) distortion, and of the effect of resonant scattering on the thermopower at 300 K. (a) Background DOS (orange) and total DOS after Lorentzian distortion added (black), in following calculations it is assumed that the total DOS comes from a single, distorted band. (b) Relaxation time due to scattering of electrons by acoustic phonons (blue), resonant scattering with $\tau_0 = 10^{-12}$ s (brown) and $\tau_0 = 10^{-13}$ s (red) and total time for those cases, (c) Thermopower at 300 K for the background DOS (orange), background DOS with acoustic phonon scattering (blue) and distorted DOS with acoustic phonon scattering (black). (d) Thermopower at 300 K for the background DOS with acoustic phonon scattering (blue) and its modifications due to resonant scattering with $\tau_0 = 10^{-13}$ (red) and $\tau_0 = 10^{-12}$ (green). (e) Comparison of the thermopower at 300 K as a function of carrier concentration for: background DOS with acoustic phonon scattering (blue) and its modifications by resonant scattering or DOS distortion effects. In all cases DOS distortion gives the highest increase in S over the broad energy and carrier concentration range. Figure taken from **[H3]**.

systems with resonant impurities were focused on, in the case of semiconductors is important mainly at low temperatures, where it can also lead to an increase in S. At high temperatures, however (in practice already near room temperatures), due to the domination of electron-phonon scattering, resonant scattering ceases to be dominant for the thermoelectric properties. It is crucial that the peak

in the density of states does not come from an additional impurity band, but it has to be the effect of modifications of the original valence (conduction) band in the material. At that time it was not yet clear whether such a situation occurs in reality and my further works **[H4]**, **[H6]**, **[H5]** and **[H8]** showed how to solve this problem and confirm that in PbTe:Tl the impurity band does not form, whereas it can be formed eg. in PbTe:Ti.

In addition, for the purpose of this work I carried out a new analysis of my results of calculations of the electronic structure for the PbTe semiconductor doped with thallium and performed approximate calculations of thermopower based on the density of states and taking into account the correction for electron-phonon scattering (details in the publication). Surprisingly well, calculations for $Tl_{0.02}Pb_{0.98}$ occurred to be quantitatively consistent with the measurements, proving the positive role of resonance for thermoelectric properties and predicting large value of S. This was the first quantitative confirmation of the thermopower boost by the resonant state, based on the it ab initio calculations. Simplified, because it was based on the approximate formula for thermopower (Sommerfeld expansion of the 2nd order) and the density of states function, not the transport function (hence the scattering effects are not accounted for). These limitations were only removed in the later work **[H12]**, where the problem of carrier concentration in the material was also solved. These will be described in more detail in the description of the **[H12]** publication.

In the paper **[H3]**, the first results of calculations of density of states for material contrasting with PbTe:Tl, namely for PbTe doped with titanium (Ti) are also presented. Titanium also exhibits resonant dopant properties [19], whereas no effect of presence of Ti on the thermopower of the system [19] were found. The analysis of partial densities of states performed in this study showed significant differences between the resonant states of thallium and titanium, supporting earlier conclusions included in the discussion in the paper **[H1]**. The resonant state induced by thallium atoms arises on states with symmetry s (orbital momentum momentum $l = 0$). At 2 % thallium concentration in PbTe resonance states hybridize with electron states of the PbTe crystal and, as a result, the density of electron states at the Fermi level mainly consists of p-states ($1 = 1$) of tellurium and lead atoms, with only about

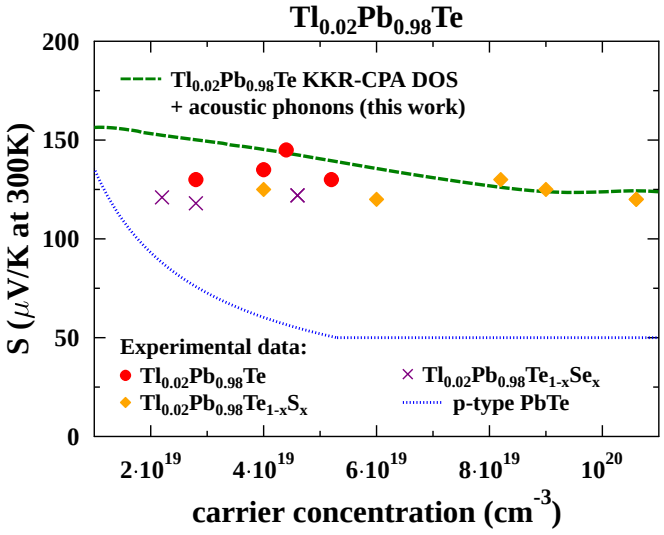

Figure 5: Thermopower in PbTe doped with 2% Tl, calculated using the density of states, obtained by the KKR-CPA method, and taking into account the correction for scattering on acoustic phonons (green line). Points show experimental data from [5] and **[H1]**. The blue line shows the reference thermopower of PbTe as a function of the carrier concentration for the material without resonant dopants.

10% contribution from thallium resonant states. This shows a significant degree of hybridization, suggesting the delocalization of electron states in PbTe:Tl. In contrast, in PbTe doped with titanium the situation is completely different, the resonant state is formed on the 3d states ($1 = 2$) of titanium, which dominate in the density of electron states of the doped system (contribution of 50%). In addition, for 3d states, which have a stronger tendency to localization, it is suspected that they can form an independent impurity band, very narrow (with a small dispersion), which implies a high density of states but also a small conductivity (large effective mass). In this case, the total thermopower of the material S is the weighted average thermopower of the matrix material's band S_m (PbTe) and dopant band S_r (Ti), where the weights are the electron conductivities of the bands:

$$S = \frac{\sigma_m S_m + \sigma_r S_r}{\sigma_m + \sigma_r}. \tag{5}$$

When $\sigma_r \ll \sigma_m$, weighted average gives $S \simeq S_m$, and there is no positive eddect of resonance on the thermopower. Such a result was observed in the measurements for PbTe:Ti – the thermopower of the material did not differ from PbTe doped with other n-type dopants. Analysis based on the density of states, suggesting poor hybridization of dopant states with PbTe matrix states suggests the scenario of forming a narrow impurity band in PbTe:Ti, which explains the lack of influence of resonant states on thermopower in n-type PbTe. The above analysis allowed to formulate another criterion, which should be followed when looking for potential "useful" resonant dopants for TE material - electronic states forming resonance should have the same symmetry as electronic states of the host material. That is, in typical semiconductors one should look for resonances on s or p electrons (with orbital quantum numbers $1 = 0$ or 1), which distinguishes them from known metallic alloys, where resonances from states of d ($l = 2$) states are important for their thermoelectric properties.

The analysis, based on the density of states, is not yet a definite proof of the hypothesis of forming (or not forming) impurity bands and hybridization tendencies. This problem, on the example of Tl and Ti doped PbTe, was the subject of my further works, i.e. **[H4]** and **[H5]**, and the results of these two works were directly compared in the short review paper **[H8]**, which will be described later in this document.

[H4] B. Wiendlocha, "Fermi surface and electron dispersion of PbTe doped with resonant Tl impurity from KKR-CPA calculations", Physical Review B **88**, 205205 (2013).

Since the calculation of the density of electronic states does not allow to directly investigate how the doping modifies the electronic bands in the material, it was necessary to extend the research to investigate the modifications of the electronic dispersion relations. The difficulty is that in the doped material chemical disorder appears, i.e. Bloch's theorem is not valid, and in general the electronic bands are not longer well-defined. In the KKR-CPA method, the translational symmetry disorder is "removed" by the coherent potential approximation (CPA), thanks to which the chemically disordered alloy is represented by an ordered medium, composed of "effective" scattering centers, described by the self-consistent, effective Green's functions [13, 14, 17]. This allows one to perform calculations in a single unit cell of the material, without the need for building large super-cells. Thanks to the knowledge of the Green's function, it is possible to directly determine the density of states (related to the integral of the imaginary part of the Green's function). The problem of how the electronic bands change requires using a more general quantity, which is the Bloch spectral function $A^B(\mathbf{k}, E)$ (BSF). BSFs are

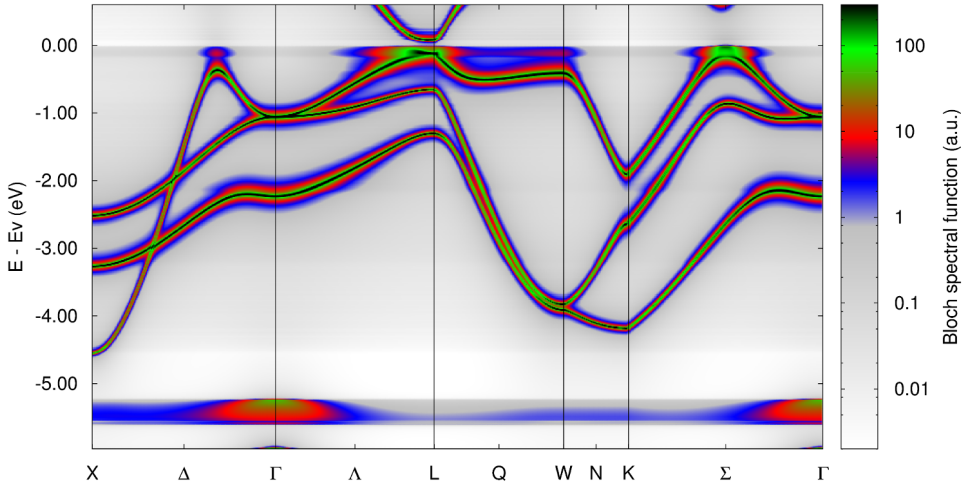

Figure 6: Bloch spectral functions of $Tl_{0.02}Pb_{0.98}Te$ plotted in log scale, with the value represented by a color. The BSF of "hyper-deep" state around -5.5 eV is visible, and resembles the isolated impurity band, in contrast to the RL located close to the valence band edge, which 'blurs' the original band.

related to the Fourier transformed configurationally averaged electron's Green's function:[20, 21, 17]

$$A^B(\mathbf{k},E) = -\frac{1}{\pi N}\sum_{i,j}^{N} e^{i\mathbf{k}(\mathbf{R}_i-\mathbf{R}_j)} \times \text{Im Tr}\int_\Omega d^3r \langle G(\mathbf{r}+\mathbf{R}_i,\mathbf{r}+\mathbf{R}_j)\rangle \tag{6}$$

where i,j are lattice site indices, and Ω the unit cell volume. More intuitively, $A^B(\mathbf{k},E)$ is a $\mathbf{k}$-resolved density of states $n(E)$ [20], since

$$n(E) = \frac{1}{\Omega_{\text{BZ}}}\int_{\Omega_{\text{BZ}}} d^3k A^B(\mathbf{k},E). \tag{7}$$

For the ordered system, BSF at selected $\mathbf{k}$ is a Dirac delta function $\delta(E-E_{\nu,\mathbf{k}})$, being zero everywhere except the points $(\mathbf{k},E)$, where electron in band ν has an energy eigenvalue $E_{\nu,\mathbf{k}}$. An integral of BSF over the energy is equal to one – each $|\mathbf{k}\rangle$-state is occupied by one electron (or two, due to spin degeneracy in the case of a non-magnetic system). In this case, a set of BSFs along selected $\mathbf{k}$-path defines the usual dispersion relations, with peaks of $\delta(E-E_{\nu,\mathbf{k}})$ functions showing the position of the ideally sharp bands $E_\nu(\mathbf{k})$, with infinite lifetime of electronic states, as no scattering takes place. In a case of a disordered system, electrons are scattered, thus BSF broadens, leading to blurring of energy bands, and decreasing the electronic life time. Typically, due to broadening of the δ-function, BSF at a single $\mathbf{k}$-point adopts the Lorentzian shape [22, 6, 23]

$$A^B(\mathbf{k},E) = L(E) = \frac{1}{\pi}\frac{\frac{1}{2}\Delta}{(E-E_0)^2+(\frac{1}{2}\Delta)^2}, \tag{8}$$

where Δ is the full width at half maximum (FWHM), representing the bandwidth, and E_0 is the Lorentzian peak position, which defines the band center. The electronic life time is then calculated as $\tau = \hbar/\Delta$. In the presence of strongly scattering impurities, which is the case of resonant impurities, spectral function becomes very wide and non-Lorentzian in shape, as it may even become impossible to point the energy band center.

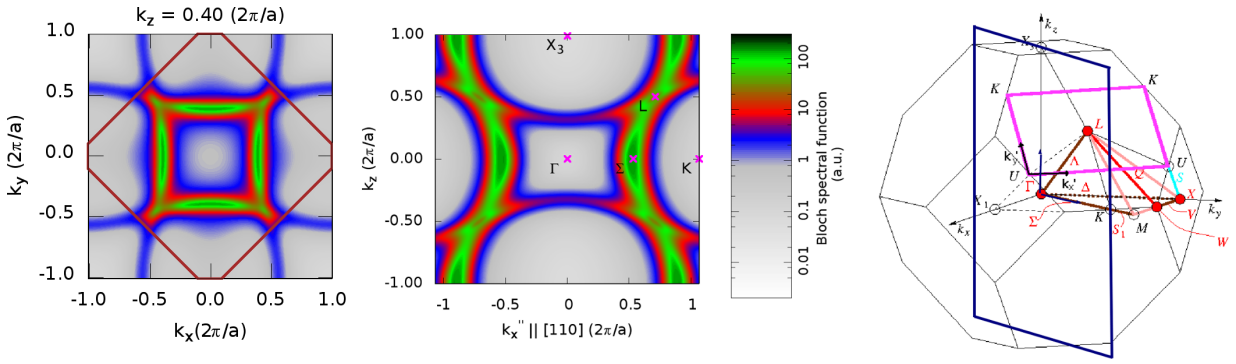

Figure 7: Cuts through the Brillouin zone, showing the smeared Fermi surface in PbTe doped with 2% of Tl. The resonant-induced "cloud" of electronic states, which are filling the tubes of the original Fermi surface of PbTe, going between L and Σ points, are visible. Picture on the left is a xy cross-section, for $k_z = 0.40\ (2\pi/a)$, middle picture is a cut parallel to [110] direction, marked as a navy rectangle in the Brillouin zone picture on the right.

In the paper **[H4]** the formalism of spectral spectral functions was used to examine the influence of Tl dopants on electronic bands and Fermi surface of PbTe. This was the first example of application of this formalism, originally developed for the study of metallic alloys, to the case of a doped semiconductor. The results demonstrated for the first time that Tl does not form a local impurity band near the edge of the valence band, which we previously suspected on the basis of DOS, and now there was a direct confirmation. This issue was very important since the arguments put forward by researchers skeptical about the idea of a resonant increase in thermopower, based mainly on the argument of creating a narrow impurity band, and as a result, removing the effect of resonance on thermopower by the weighted average in the equation 5. The more that in previous work [24], calculations based on the supercell technique, directly claimed the formation of the impurity band in PbTe:Tl.

KKR-CPA calculations showed a different effect – through its resonant character, Tl admixture leads to a very strong blurring of the highest valence band in PbTe. This blurring, visible as a significant widening of the spectral functions, is so strong that there is no well-defined valence band in PbTe:Tl anymore (this will be particularly well seen in Fig. 19 from work **[H12]**, described later). Consequently, the Fermi surface of PbTe:Tl is made up of tubes that are "filled" with additional electronic states, compared to the respective structure of pure PbTe. Plots of spectral functions and example of the fuzzy Fermi surface cross-section are shown in Fig. 6 and 7, more in **[H4]** paper.

As shown by the analysis of atomic contributions to the spectral functions, additional electronic states appearing around the original valence band are highly hybridized states with the highest contribution from the Te atoms, which confirms that Tl resonant states act as a kind of catalyst, shifting electronic states from deeper energy regions towards the edge of the band, where they can contribute to transport phenomena. This allowed me to propose a new interpretation of the effect of resonance on the thermopower: those additional electronic states affect the transport properties of the system in a manner analogous to the effect of increasing the bands degeneration (an effect analogous to the so-called convergence of bands), which is a recognized factor that increases the thermopower of the system. Drawings of spectral functions from this work were recognized by the presentation in the it Kaleidoscope section on the main page of the Physical Review B.

[H5] B. Wiendlocha, "Localization and magnetism of the resonant impurity states in Ti doped PbTe", Applied Physics Letters **105**, 133901 (2014).

The interesting results of the application of Bloch spectral functions formalism for analyzing the problem of resonant states and the formation of impurity bands, obtained in [**H4**], prompted me to apply these methods to other cases. Another analyzed example was PbTe doped with titanium, which was used in the previous work [**H3**] as a counter-example of a system containing a resonant impurity, which did not improve the material's thermopower. In the work [**H5**] KKR-CPA calculations of density of states, magnetic moments, and Bloch spectral functions were performed for PbTe doped with 2% Ti. The previous results of my calculations of electronic density were confirmed, with a very narrow, resonant DOS peak showing the resonant character of the Ti dopant. The DOS peak is so high that there is a magnetic moment on Ti atoms, equal to about 1.6 μ_B. The results of calculations of spectral functions confirmed earlier speculations, that Ti resonant states tend to localize, because the spectral function associated with them does not show dispersion as a function of the wave vector $\mathbf{k}$. In Fig. 8 it can be seen in the form of narrow "impurity bands" associated with the split $3d-e_g$ and $3d-t_{2g}$ states of titanium. Such flat bands describe strongly localized states, because their effective mass m^* will be very large, due to the lack of curvature of the band. Thus, in this case, the scenario of forming a narrow impurity band is realized, thus the thermopower does not "see" the resonance effect due to the small conductivity of the impurity band. This example contrasts with the case of PbTe:Tl, where the spectral functions predicted delocalization and hybridization of resonant states. The spectral functions for both of these systems are plotted in Fig. 8, taken from the paper [**H8**], which discusses, among others, results of [**H4**] and [**H5**] publications. In turn, Fig. 9 presents the spectral functions at the point $\mathbf{k} = (0, 0, 0)$ (Γ point), where the contributions to the BSF were also drawn from individual crystallographic positions, i.e. (4a), occupied by Pb and Ti, and (4b), occupied by Te. One can see that the original PbTe band below E_F comes from hybrid states from both positions (contributions from Pb and Te), while states appearing above E_F, associated with resonance, will come from unhybridized Ti states, because at the Γ point, in this energy range, there is no band in PbTe (hence the only contribution will be from Ti).

These results confirmed, that for a resonant state to be successful in improving the thermoelectric properties of a material, it is necessary to hybridize with the electronic states of the host material, and that it cannot form narrow impurity bands. Qualitative explanation of the difference between PbTe:Tl and PbTe:Ti has also shown, that the Bloch spectral functions technique may be successfully applied to investigate the localization and impurity bands formation tendencies in the semiconductor thermoelectric materials.

[**H6**] S. Kim, B. Wiendlocha, H. Jin, J. Tobola, J.P. Heremans, "Electronic structure and thermoelectric properties of p-type Ag-doped Mg_2Sn and $Mg_2Sn_{1-x}Si_x$ ($x = 0.05, 0.1$)", Journal of Applied Physics **116**, 153706 (2014).

This work emerged as a result of the theoretical-experimental cooperation as part of the project of searching for new resonant impurities in TE materials, in this case in the alloys based on Mg_2Sn and Mg_2Si compounds. The introduction to this work were theoretical calculations of electronic densities of states for many potential impurities that could be substituted for Mg or Sn in the Mg_2Sn system. As a result of this "screening", we focused on the Ag doping, for which the DOS calculations and then the BSF showed that in the situation where Ag substitutes the Sn atom, it can lead to the formation of a (delocalized) resonant state (i.e. not forming a narrow impurity band). Additionally, Ag should be a p-type dopant, especially sought after in the systems of Mg_2(Sn-Si). To verify the predictions, the experimental group from OSU synthesized a series of samples of Mg_2Sn and $Mg_2Sn_{1-x}Si_x$,

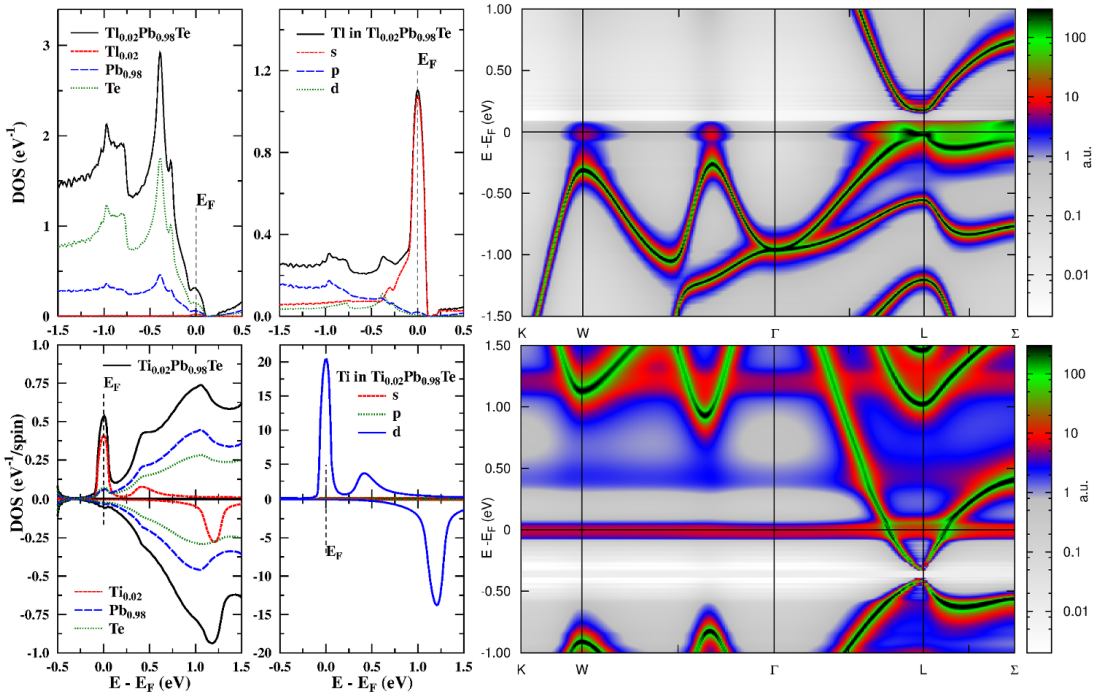

Figure 8: Contrast between spectral functions and densities of states of PbTe doped with 2% Tl (upper panel) and Ti (lower panel). Electronic states, associated with resonance on Ti, resemble flat, narrow impurity bands, which we do not observe for Tl. The figure comes from the review paper **[H8]**, while the original results were obtained in the works **[H4]** and **[H5]**.

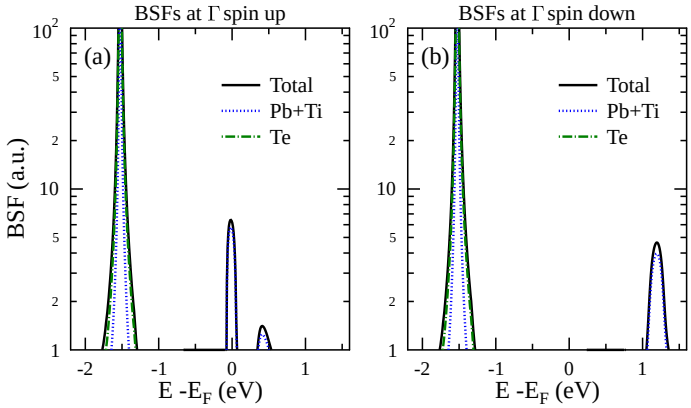

Figure 9: Bloch spectral functions for PbTe with 2% Ti, at Γ point. Color lines show contributions from crystal sites: (4a) occupied by Pb and Ti, and (4b) occupied by Te. The two peaks above 0 eV for spin-up and one for spin-down channels originate from the impurity states, and show no hybridization with Te states. The peak around -1.5 eV comes from the original PbTe band.

($x = 0.05, 0.10$) doped with Ag, and performed measurements of the transport properties. The measurements confirmed the acceptor character of Ag, but unfortunately did not show a resonant effect of increasing the thermopower - points on the Pisarenko curve for the studied materials were in line with the predictions for regular dopants in Mg_2 Sn (figure 9 in the publication). To understand the reason for this effect, I extended the calculations for Ag located in the Mg position, which was additionally suggested by independent theoretical work [25], and experiment [26], where in the sister system Mg_2Si it was found that the Ag atoms may also substitute the Mg position or leave the Si position at higher

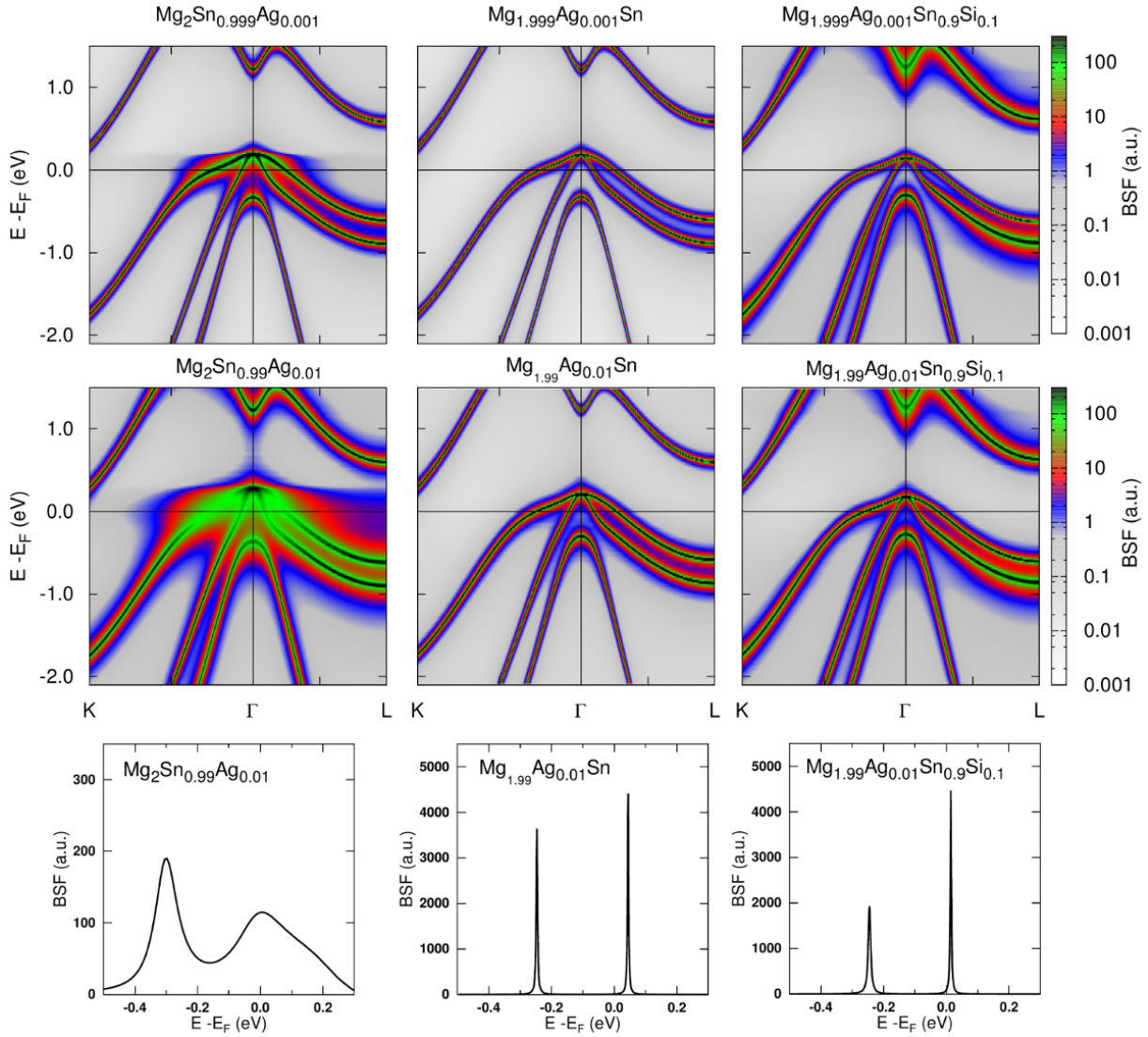

Figure 10: Comparison of the Bloch spectral functions for the 3 studied cases. When Ag substitutes Sn (left column, $Mg_2Sn_{0.99}Ag_{0.01}$ it shows resonant behavior, strongly blurring BSF. For the Ag on Mg position, ($Mg_{1.99}Ag_{0.01}Sn$, middle column), it behaves as a rigid-band-like impurity, only shifting E_F. Addition of Si on Sn site (right column) leads to a small broadening of BSF due to an additional alloy scattering. In all the cases, Ag is a p-type dopant. Bottom panel shows the spectral functions for $\mathbf{k} = (0.115, 0.115, 0.115)$ $2\pi/a$, where strongly distorted BSF for the resonant Sn/Ag doping case are seen,in contrast to minor BSF widening for the Mg/Ag substitution case.

temperatures. In addition, the specifics of the synthesis conditions of the aforementioned compounds (i.e. the need to add excess Mg to the ampoules during synthesis due to the evaporation of Mg) does not allow for intentional doping at a given crystallographic position by controlling the amount of materials used for synthesis. The calculations showed that in the case of the Ag atom locating at the Mg position, there is no resonant state formation, as shown in Fig. 10. This explains the "regular" effect of Ag on the thermopower, only by changing the carriers concentration in the rigid band style, without resonant raise of S. This allowed us to classify Ag as a "regular" acceptor in $Mg_2Sn_{1-x}Si_x$, ($x = 0.00, 0.05, 0.10$), which most likely substitutes Mg atoms.

[**H7**] H. Jin, B. Wiendlocha and J. P. Heremans, "P-type doping of elemental bismuth with indium,

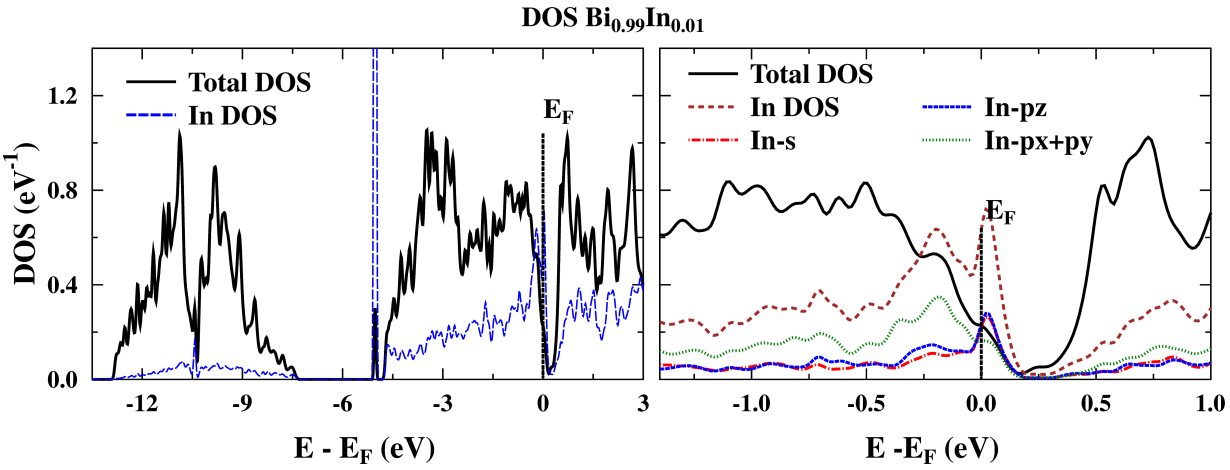

Figure 11: Calcluated density of states for $Bi_{0.99}In_{0.01}$. Separated DOS peak is formed below the main valence band, around -5 eV below E_F. Near E_F In impurity does not markedly modify the electronic structure of the system.

gallium and tin: a novel doping mechanism in solids" Energy & Environmental Science **8**, 2027 (2015).

This work is a continuation of the project of searching for resonant impurities in the Bi and Bi-Sb system for applications in cryogenic thermoelectric coolers. Quite unexpectedly, it resulted in the identification of a new doping mechanism, through the creation of a deep resonant state, thanks to which the atom, isoelectronic with the substituted one, can become an electrically neutral acceptor (although this statement seems to be internally contradictory). Thanks to such an unusual doping mechanism, it is possible to avoid scattering of carriers on the ionized impurities, as the dopant atom is electrically neutral with respect to the substituted atoms. The publication is very extensive, it contains an experimental and theoretical part, where calculations were carried out with two complementary methods to mutually verify the results, which is why only the most important results will be quoted here. In the case of this work, the beginning of the study was experimental screening (OSU group), where transport measurements were performed on a series of polycrystalline Bi samples containing various dopant atoms. The indium-doped system was selected for further studies on monocrystalline samples. In addition to interesting transport properties, what caught our attention was the acceptor behavior of indium, which is a trivalent atom, as well as bismuth. It should therefore be an electrically neutral impurity, while measurements of the Hall and Shubnikov-de Haas effects clearly showed an increase in the concentration of holes after the substitution of In. My theoretical calculations showed that In does not create resonant state near the Fermi energy in Bi, but creates a deep resonant state (so-called HDS, hyper-deep state) with energy around -5 eV below E_F, as shown in Fig. 11. A similar HDS state is formed in PbTe: Tl (and several other materials with resonant states), but always combined with resonance at E_F. Here, in Bi:In, around E_F the behavior of In only slightly differs from the regular shifting of E_F, as for the "regular" acceptor, almost in line with the rigid band model.

Analysis of the charge density around the In atom, associated with the HDS peak, showed that this state is a bound state, formed between one 5s In electron and one 6p Bi electron, which in 1/6 comes from from each of the 6 Bi atoms, which are nearest neighbors of In.[1] This bonding can be seen in the Figure 12 of the charge density for a plane containing 4 out of 6 In neighbors (the plane

[1]In a rhombohedral bismuth cell, a substituted In atom has 3 nearest and 3 next nearest neighbors in the form of Bi atoms, NN are 3.06 Å, and NNN 3.46 Å from In, respectively. These numbers take into account the relaxation of the crystal structure around the In atom.

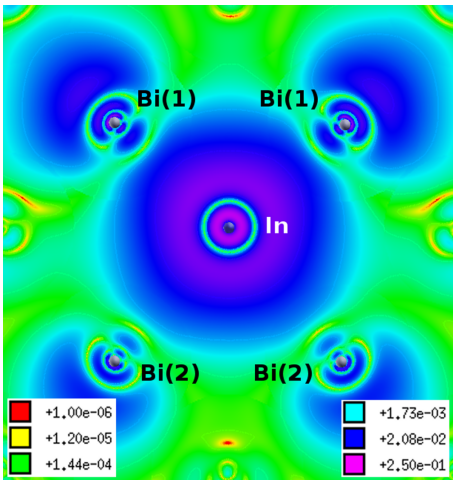

Figure 12: Color map of the charge density in (e/Å^3) in logarithmic scale around an In impurity, corresponding to the hyperdeep defect state (HDS) peak. The nearest Bi(1) and next nearest Bi(2) atoms are labeled. One can see the bonding between 5s In and 6p Bi states.

is shown in Figure S3 in the supplemental material of the publication). Thus, this local bound state "extracts" one Bi electron from the valence band, also binding one In electron. Thus, the original trivalent In atom, after substituting for Bi, causes two holes to appear in the valence band. This explains the acceptor behavior In in Bi [2], constituting a new mechanism of materials' doping – not by introducing an electrically active atom with a different number of valence electrons, but by creating a deeply located resonant state that "deactivates" some of the electrons in the system. Such a doping mechanism, observed here for Bi:In, is associated with one very advantageous feature, namely the lack of scattering of carriers on the ionized impurities. Since In and Bi have the same number of valence electrons, then from the point of view of the charge carriers in the system, the In atoms remain electrically neutral. This effect can be experimentally captured by analyzing temperature dependence of conductivity and thermopower in the material. Such analysis has been carried out and confirmed the occurrence of scattering on neutral impurities, which is an independent confirmation of the proposed doping mechanism. This type of scattering is particularly advantageous for thermoelectric materials because, firstly, it does not cause such a reduction in mobility of carriers as scattering on ionized centers, and secondly it gives larger thermopower while compared to the most common case with scattering on acoustic phonons (which reduces S).

To verify our hypotheses, similar calculations and measurements were done for Ga doped Bi (Ga is isoelectronic with In), and Sn doped Bi (Sn has one valence electron more than In). For Ga, as expected, both calculations and measurements showed identical effects of the "neutral acceptor", with formation of the HDS state, that we observed for In. Quite unexpected results appeared in the case of Sn, which was considered for decades to be a typical one-hole regular acceptor in Bi (interestingly, at that moment no theoretical calculations for doped Bi were published). It turned out that the mechanism of the acceptor behavior of Sn in Bi is also based on the creation of a local, bound HDS state between one 5s electron of Sn and one 6p electron of Bi, with the ideal rigid-band-like dopant behavior at the Fermi level (see Figure 5 in the publication). Since Sn has one valence electron more than In, it behaves like a one-hole acceptor, in perfect agreement with the experimental results (here, there is no problem of low dopant efficiency, which we explained for In by the presence of interstitial atoms).

[2]The experimentally measured doping efficiency was not so large, which we explained by partial compensation of holes due to location of some of the In atoms in the interstitial sites

However, the difference in the number of valence electrons (4 in Sn, 3 in Bi) makes Bi:Sn an ionized impurity, thus no neutral impurity scattering effects were observed.

[H8] B. Wiendlocha, K. Kutorasiński, S. Kaprzyk, J. Tobola, "Recent progress in calculations of electronic and transport properties of disordered thermoelectric materials", Scripta Materialia **111**, 33 (2016).

This work is largely a review work, where the most important results, recently obtained in the "band-structure team" in KFMS WFiIS AGH, were collected and discussed. This work contains four paragraphs: *1. Resonant levels*, *2. Bands convergence*, *3. Bands alignment*, *4. Spin-orbit interaction*. I'm the author of paragraph 1., and partially 4. In §1, concerning resonant states, I have included previously unpublished results of density of states calculations for 0.1 % Ni-doped Cu, Sn in Bi_2Te_3 and In in SnTe, confirming the formation of resonant states at the dopant atoms in the above mentioned systems, in agreement with experimental results. As I mentioned above, the results of the works **[H4]** and **[H5]** (Fig. 8), showing the differences in resonant Tl and Ti behavior in PbTe, were collected here (delocalization and hybridization for Tl, and creation of a narrow, localized impurity band for PbTe:Ti). In addition, I carried out part of the calculations described in §4, where the influence of spin-orbit coupling on thermopower in Mg_2X (X = Si, Ga, Sn) was investigated.

[H9] B. Wiendlocha, "Resonant Levels, Vacancies, and Doping in Bi_2Te_3, Bi_2Te_2Se, and Bi_2Se_3 Tetradymites", Journal of Electronic Materials **45**, 3515 (2016).

This work presents the results of theoretical investigations on resonant impurities and interactions of resonant states with defects and other dopant atoms in the family of tetradymites based on bismuth: Bi_2Te_3, Bi_2Te_2Se and Bi_2Se_3. Tetradymites are the family of extremely interesting compounds, which are the best thermoelectrics for applications in the region of room temperatures, and at the same time showing topological properties of surface states. The direct reason for my interest in these systems was the earlier, experimental observation of the resonant state on Sn atoms in Bi_2Te_3 [27], with a nearly doubled thermopower for carrier concentrations around $p = 5 \times 10^{19}$ cm^{-3}. The first theoretical calculations, confirming the formation of the resonant state on the 5s states of tin atoms in Bi_2Te_3 I made while working on **[H8]**. Here, the evolution of the resonance with the increasing concentration of Sn was investigated, and the effect of the crystal lattice relaxation and the spin-orbit coupling on the Sn resonance was investigated in this system. It turned out that RL on Sn is insensitive to the local distortion of the crystal lattice around the dopant atom, and that the spin-orbit interaction does not directly affect the resonance, which is understood due to its orbital character (s-like states).

In the next step, I analyzed whether Sn forms resonant states in other Bi-based tetradymites. The KKR-CPA calculations showed that the resonant state should also be created in the valence band of Bi_2Te_2Se and Bi_2Se_3. The acceptor character of the Sn dopant is important here, because both compounds are characterized by a much more complex and more difficult to control defect chemistry than Bi_2Te_3 [28]. This is why for many years in both cases, only n-type samples were available in experimental studies, most likely due to formation of vacancies on Se or Te sublattices. A little earlier, the experimental paper [29] was published, in which the influence of Sn doping on the thermoelectric properties of Bi_2Te_2 Se was investigated. Since the unopened samples, due to the presence of vacancies, were n-type, the authors had to strongly dope the system with Sn to obtain p-type samples. For 1% Sn doping, compensation of defects was reached, and 4% Sn-doped sample was p-type, which, however,

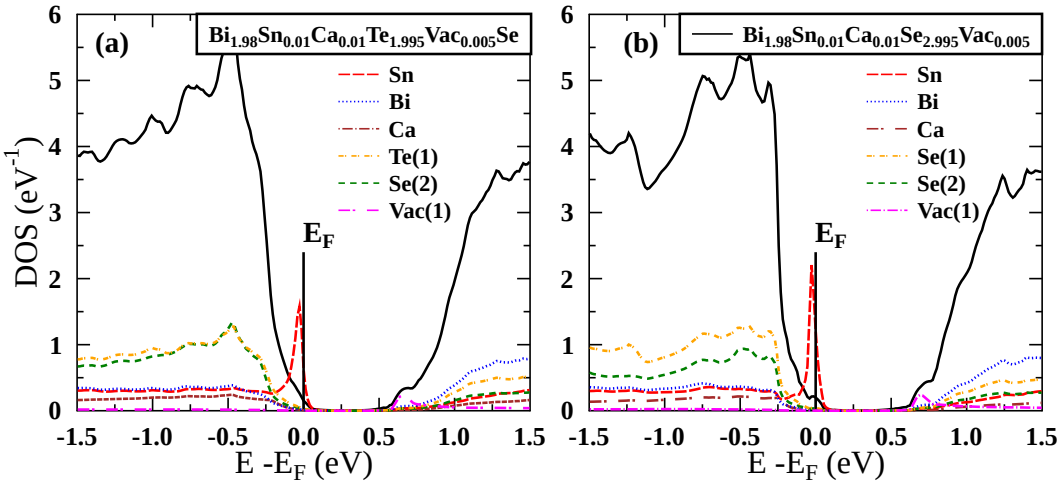

Figure 13: DOS of the doubly, Sn- and Ca-doped (a) Bi_2Te_2Se, and (b) Bi_2Se_3, both containing 0.5% of the outer-layer vacancies Vac(1). Our results show that the double doping, using a rigid-band-like acceptor (here Ca), should be an effective way of tuning the Fermi level position, without broadening the Sn RL too much.

did not show any "resonant" features for thermopower. To explain the possible cause of this fact, and to examine how vacancies affect the formation of resonant states, I performed calculations for a system containing simultaneously, Sn atoms in the Bi position, and vacancies on the Se and Te sub-lattices. The results of KKR-CPA calculations showed that regardless of the location of the vacancy (any of the two, non-equivalent Se positions in Bi_2Se_3, or Se and Te sub-lattices in Bi_2Te_2Se), they behave like a two-electron donors, creating a n-type material, and that resonant state on Sn is formed also in the presence of vacancies. The calculations confirmed that with the concentration of the defect, suggested by experimental studies (0.5 %), 2x more atoms of Sn (one-hole acceptors) are needed to compensate for the effect of the vacancy and to place the Fermi level in the gap. For higher Sn concentrations, the system becomes a p-type semiconductor, but the resonance state is also remarkably blurring. For 4% – the concentration of Sn used in the cited experiment – the resonant state may already be so blurred that it explains the observed lack of resonant increase in thermopower. It is worth noting here that in the Bi_2Te_3 system with a similar concentration of Sn (5%), the impact of resonance on the thermopower was also not significant anymore, with the best results obtained for 1% - 2% Sn concentrations. Unfortunately, in Bi_2Te_2Se, the need to compensate donor states caused that concentrations of Sn used in the experiments were much higher, which could have caused too much blurring of the resonant state and, consequently, no clear effect on the thermopower. In the work I suggested how one can potentially avoid the above-mentioned problem by using a second dopant. Calculations for a quite complicated case with two types of dopants and vacancies have shown that the resonant state also forms when there is a double doping in the material. Thanks to this, one type of impurities (regular ones, like Ca or Mg) may compensate for the donor effect of the vacancy, which will allow obtaining a p-type sample for 1% - 2% concentration of the second, resonant dopant Sn. A variation in the concentration of the second, regular dopant atoms will allow to scan the DOS resonant peak, without the need for too large concentration of Sn. Example result for double doped (1% Sn and 1 % Ca) Bi_2Te_2Se and Bi_2Se_3, containing 0.5 % of the vacancy, is shown in the figure 13. The resonance peak from Sn in the vicinity of E_F is visible, where at the same concentration of Sn, and without the presence of Ca, the Fermi level is in the gap. In the last part of the work, I published the results predicting the possibility of creating a resonance state on the Ga and Al atoms in the entire tetradymite series under

study, to encourage experimental groups to undertake research on these dopants.

[H10] J.P. Heremans, B. Wiendlocha, H. Jin, Thermoelectric Materials with Resonant States, rozdział w monografii *Advanced Thermoelectrics: Materials, Contacts, Devices, and Systems*, ed. Z. Ren, Y. Lan, Qi. Zhang, CRC Press, Taylor & Francis Group, Boca Raton, FL (USA), 2018.

This is a chapter in a monograph devoted to thermoelectric materials. In addition to the review part about resonant levels, similar to the one in the work **[H8]** (therefore it will not be reviewed again here), it contains very intriguing results that we obtained in cooperation with the OSU group for bismuth and Bi-Sb alloy doped with potassium (K). These studies were carried out as part of our project to study thermoelectrics for applications at cryogenic temperatures. The introduction to the work on potassium doping were the calculations of the electronic structure of Bi with many, previously non-studied dopants, of which potassium showed the formation of a resonant DOS peak in on p states, just above E_F (Fig. 14). The calculations were then repeated for the Bi-Sb alloy, which is the target thermoelectric material, due to the opening of the semiconducting gap. Experimental work on this material included the preparation of several single crystals of Bi-Sb with an addition of K, near the composition, for which the Bi-Sb system is a good thermoelectric. It should be noted here that the control of the growth of Bi-Sb monocrystals is quite problematic, and the obtained materials are characterized by a concentration gradient of Sb atoms along the sample, hence each of the cut-out pieces of the test sample had a slightly different composition. It turned out that all tested samples of Bi-Sb:K are of the n-type, which was advantageous due to the placement of the resonant peak just above E_F in the calculations. Part of the samples generally did not show any better thermoelectric properties than the known Bi-Sb alloys, while one of the samples showed a high (as an absolute value) thermopower and high electrical conductivity, resulting in an unusually high power factor, up to 2.5x higher, than in the any other samples and reference Bi-Sb alloy, leading to 50% higher zT coefficient in the temperature range 100 K - 300 K (see, Fig. 15). This unusual discovery initiated further intensive work (theoretical and experimental) on Bi and Bi-Sb doped with K. These results were presented at several conferences, including [30, 31, 32].

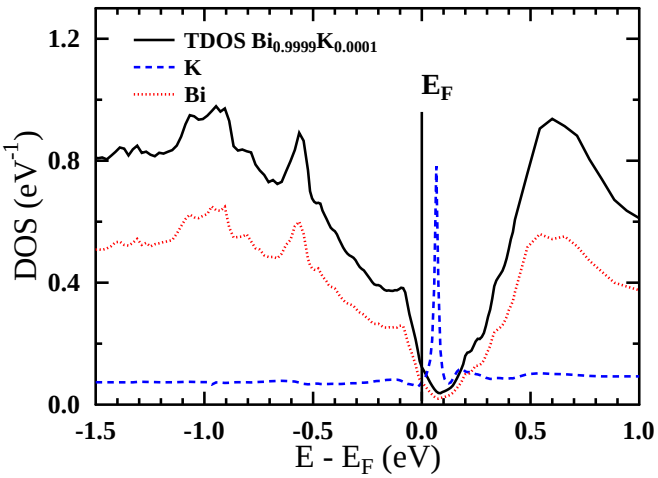

Figure 14: Density of states for K-doped Bi, showing the formation of the resonant state just above E_F.

Unfortunately, problems appeared at a later stage of experimental work in the synthesis of subsequent samples. Difficulties in controlling the composition (both Bi:Sb stoichiometry and the amount of

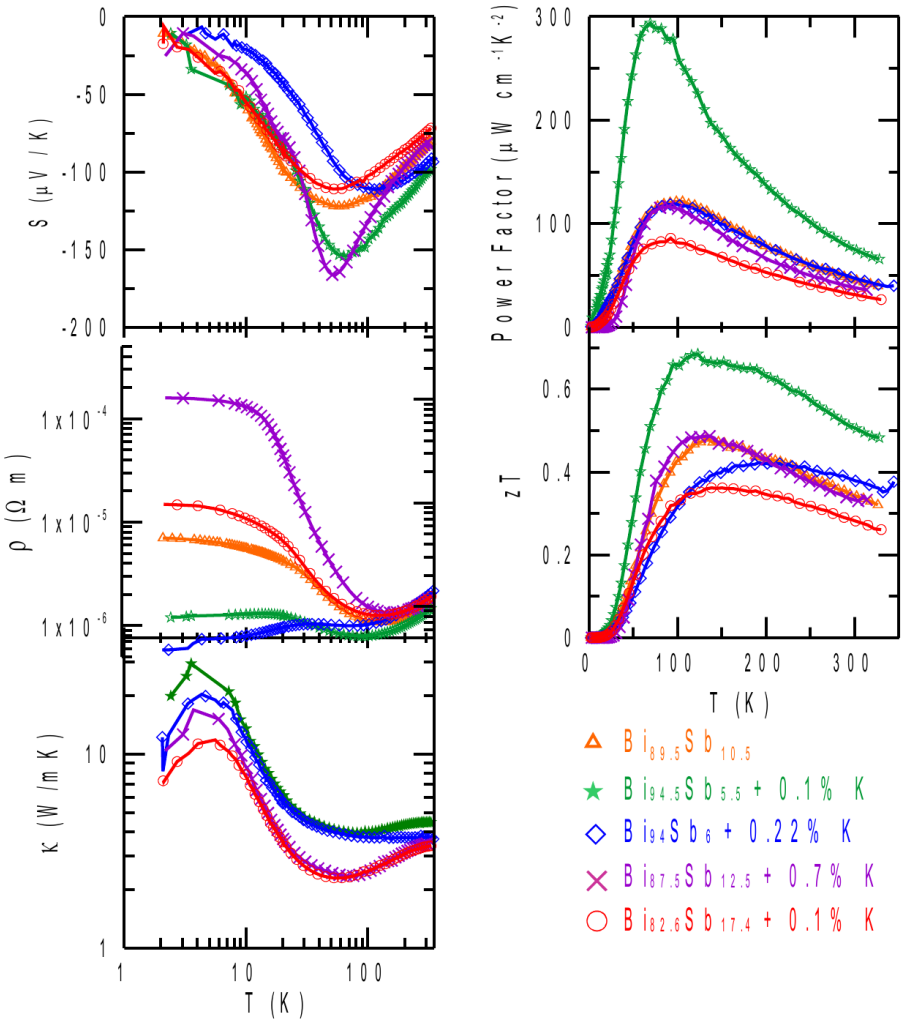

Figure 15: The results of measurements of transport properties of several samples of Bi-Sb with K dopants. The best of the samples (green) showed very good thermoelectric properties, attributed to the resonant state on K atoms.

K, which is a sticky paste) did not allow for repeatable synthesis of samples with such good properties as the first one tested, and after several months, further works were stopped. At the moment, there is therefore no unambiguous confirmation whether the resonant state on the K atoms exists in Bi-Sb alloys. The fact is that the K-doped samples had special transport properties, one of the samples was characterized by a record-high zT factor, and the calculations, also carried out using complementary to KKR-CPA methods, predict the occurrence of a resonant state. Further experimental work is necessary to resolve this issue.

[H11] B. Wiendlocha, J-B. Vaney, C. Candolfi, A. Dauscher, B. Lenoir, and J. Tobola, "An Sn-induced resonant level in β-As_2Te_3", Physical Chemistry Chemical Physics **20**, 12948 (2018).

This work was done in cooperation with the experimental group of prof. B. Lenoir from Ecole des Mines in Nancy and extends research on resonances in tetradymites on less-known system As_2Te_3 in the β phase, in which it has a crystalline structure of Bi_2Te_3. The calculations I performed for Sn-doped As_2Te_3 showed that just like in the bismuth based tetradimites (work **[H9]**) on the tin

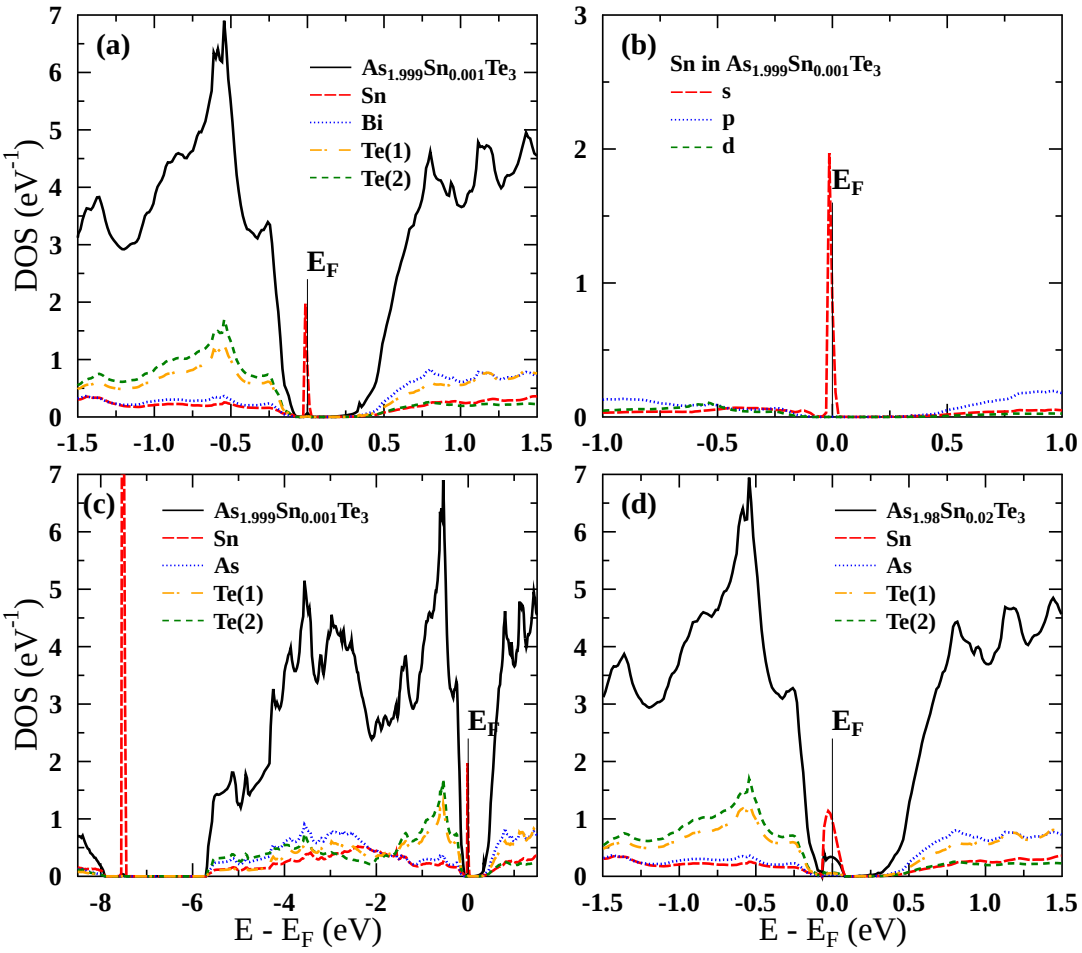

Figure 16: Energy dependence of the electronic density of states (DOS) for Sn-substituted β-As_2Te_3 for (a–c) 0.1% Sn and (d) 2% Sn, as calculated by the KKR-CPA method. Color lines show the atomic contributions per single atom (not weighted by their concentration). Panel (a) shows the position of the Sn-resonance peak at the valence band edge. Panel (b) shows the angular-momentum decomposition of the resonance peak demonstrating that it originates from the 5s orbitals of Sn. Panel (c) shows the DOS over a broader energy range, where a second, hyper-deep resonant peak is formed near -7.5 eV. Panel (d) shows the DOS for 2% Sn concentration, where the broadening and hybridization of the RL states with the host states are observed.

atom, a resonant state is formed at the edge of the valence band on 5s orbitals of Sn, as shown in Figure 16. The FP-LAPW calculations showed that, as in Bi_2Te_3, the resonant state is not sensitive to local crystal structure relaxation and the presence of spin-orbit interaction. Because the electronic structure and transport properties of β-As_2Te_3 have not been studied in detail so far in the literature, I also performed calculations of the Fermi surface, the $\sigma(E)$ transport function (in Boltzmann's approach), thermopower and Hall resistance, as a function of carrier concentration, temperature and crystallographic direction, for pristine material β-As_2Te_3. The results as a function of carrier concentration were obtained in the rigid band approximation, thus they simulate the properties of the material without resonant dopants. Calculations of the thermopower were carried out within the constant scattering time approximation (CSTA). This extended theoretical analysis allowed for a more accurate interpretation of the experimental data, and gave the opportunity to better assess the effect of resonance on the β-As_2Te_3 properties. Among other things, in the calculations, it was found that

this system shows a small anisotropy of thermopower and Hall coefficient, therefore measurements, carried out on polycrystalline samples, give a representative results, and we can neglect the impact of factors such as the texture of the samples. In addition, quite promising thermoelectric properties have been predicted for the n-type material, which has not yet been experimentally achieved.

Experimental studies were carried out on a series of samples of β-As_2Te_3 doped with Sn, Bi, Ga and I. The most important results, in the context of resonance states, are compiled on the Pisarenko curve in Fig. 17. Starting from the analysis of the results for Bi, Ga, I and one non-doped sample (self-doping via defects), it should be noted that the results of Boltzmann calculations with CSTA predict slightly higher values of S than measured experimentally. The reason for this is probably $\tau = const$ assumption, because the analysis of experimental results showed that the scattering of carriers on acoustic phonons, where approximately $\tau(E) \propto \tau_0 E^{-1/2}$ should be a dominant mechanism here. In this case, the real thermopower is lower in relation to the results of CSTA. The second of the theoretical lines in Fig. 17 was calculated in a single band model with a constant effective mass $m^*_{rmDOS} = 1.14\ m_e$, which has its justification in band calculations, and assuming $\tau(E) \propto \tau_0 E^{-1/2}$. This line determines the lower limit of the experimental results. Both approaches with fairly good accuracy describe dependence of thermopower on concentration of holes p in β-As_2Te_3. In contrast, the results for samples doped with Sn, in the range of 5-10 $\times 10^{19}$ cm^{-3} clearly show the increase of the thermopower, in relation to both calculations and measurements, for "regular" β-As_2Te_3. This confirms the formation of the resonant state on the Sn atoms in the system and its beneficial effect on the thermopower.

[H12] B. Wiendlocha, "Thermopower of thermoelectric materials with resonant levels: PbTe:Tl versus PbTe:Na and $Cu_{1-x}Ni_x$", Physical Review B **97**, 205203 (2018).

Works on the last publication included in this summary report, lasted (with intervals) definitely the longest, as the first results of calculations of transport functions in PbTe:Tl I presented in 2013 at the *32nd International Conference on Thermoelectrics* in Kobe (Japan), five years before the final publication date. This paper presents the results of calculations of transport functions, residual resistivities, carrier lifetimes and thermopower for two best-known examples of thermoelectric materials with resonant states, i.e. metallic Cu-Ni alloy (constantan), and PbTe:Tl. As a counter-example of a material without resonant state, PbTe:Na was chosen. The direct purpose of this work was to confirm the increase of the thermopower in the semiconductor containing resonant levels, by using the most accurate transport calculations possible, not based on the approximations I used earlier. For this purpose, calculations of the $\sigma(E)$ transport function were done using Kubo-Greenwood's formalism [33, 34]. The necessity to go beyond the Boltzmann formalism is caused by the fact that in systems containing resonant levels, as shown by this and earlier works, the electron bands become so blurry that pointing the "center" of the band may be impossible. This makes impossible to determine the electron velocities as well as the use of the relaxation time approximation (in particular, the most common constant relaxation time approximation is not applicable). The more general Kubo formalism, based on scattering operators, can be used in such cases, and it takes into account the scattering of carriers on dopant atoms. The resulting calculations do not contain any free parameters, giving results entirely from the first principles.

As a test material, in order to check the used procedures and gain a broader view of the resonance problem, I used a Cu-Ni metallic alloy, i.e. constantan, commonly used to build thermocouples. This material was historically one of the first in which the appearance of resonance states (here on Ni atoms) was observed [6], its analysis also shows the differences between resonant cases in the metal and semiconductor. I focused on the $Cu_{0.60}Ni_{0.40}$ composition, in which the alloy is a paramagnet and

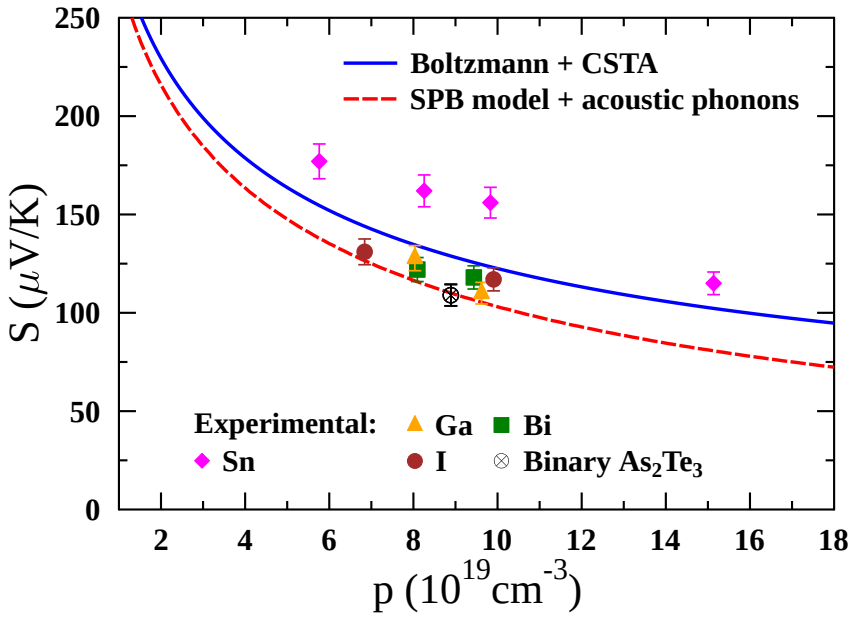

Figure 17: Pisarenko plot (thermopower versus hole concentration) at T = 300 K. The solid blue curve is computed from first principles for pristine β-As_2Te_3 within the Boltzmann approach and the constant scattering time approximation (CSTA). The dashed red line is computed using the single parabolic band (SPB) model with constant $m^*_{DOS} = 1.14\ m_e$ and assuming an energy-dependent scattering time $\tau(E) = \tau_0 E^{-1/2}$ (acoustic phonon scattering). The experimental thermopower values measured for the β-$As_{2-x}Ge_xTe_3$ ($x = 0.01$ and 0.03), β-$As_{2-x}Bi_xTe_3$ ($x = 0.015$ and 0.025), β-$As_2Te_{3-x}I_x$ ($x = 0.01$ and 0.02) series have been added for comparison with the β-$As_{2-x}Sn_xTe_3$ (x = 0.0 - binary As_2Te_3, 0.015, 0.025, 0.035 and 0.050). The increased thermopower values measured for the Sn series, with respect to other impurities and to theoretical predictions, are clearly visible. The errors bars correspond to the experimental uncertainty, estimated to be 5%.

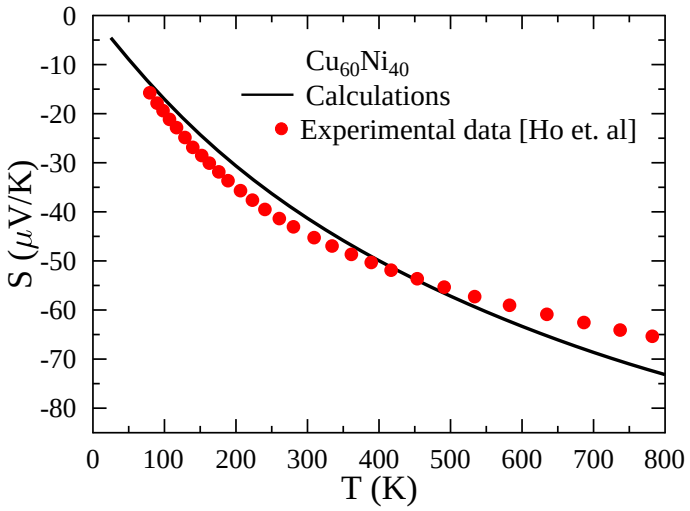

Figure 18: Thermopower of $Cu_{0.60}Ni_{0.40}$ as a function of temperature. Experimental data after Ho *et al.* [35].

has very good thermoelectric properties. Calculations of spectral functions and density of states showed the occurrence of a resonant state on the 3*d*-Ni orbitals, in agreement with previous studies [22, 36].

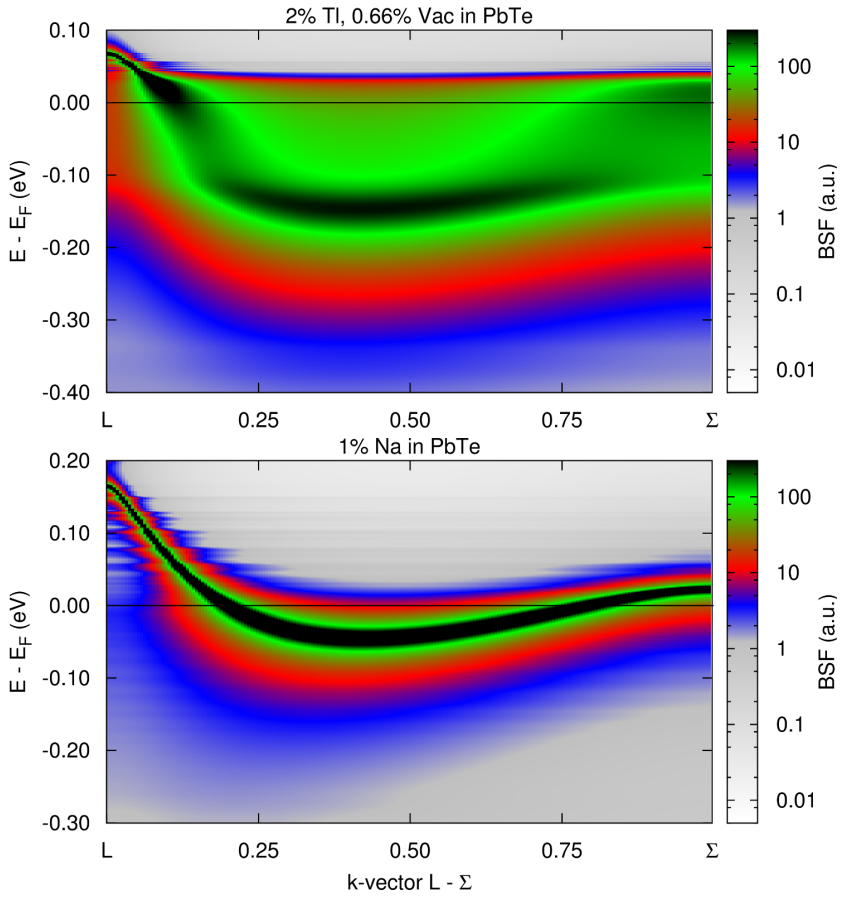

Figure 19: The two-dimensional projection of Bloch spectral functions of $Pb_{0.98}Tl_{0.02}Te_{0.9934}Vac_{0.0066}$ (top panel) and $Pb_{0.99}Na_{0.01}Te$ (bottom panel), between L and Σ points.

Calculation of the thermopower, based on the computed transport function $\sigma(E)$ gave very good results, predicting a large (as for a metal) thermopower, in very good agreement with the experimental results. For room temperature, $S_{\text{calc}} = -42$ μV/K, $S_{\text{expt}} = -45$ μV/K, and despite the neglect of the effects of scattering on phonons, up to a temperature of $T = 800$ K the agreement between calculations and experiment is better than 10 %, as shown in Fig. 18. The reason for this is the low sensitivity of the system to scattering on phonons, due to the presence of strong scattering on the resonant state, which is the dominant factor. This is confirmed by the temperature-independent resistance, in the range of 0-1000 K, changing in less than 5% [35].

Before similar transport calculations were made for PbTe:Tl, in my work I analyzed the problem of charge concentration in this system, because the measured (using the Hall effect) concentrations are much lower than the nominal [3], and thermopower fundamentally depends on carrier concentration. In the literature, this effect was explained using two models: a model with mixed Tl valence and a self-compensating model, where defects are supposed to compensate the Tl hole doping. In the work, I present a number of arguments supporting the defect compensation model, where vacancies on Te, behaving like two-electron donors, compensate the acceptor effect of Tl. In the course of the work, calculations are carried out for Tl-doped systems and simultaneously containing vacancies on the tellurium sublattice in such an amount that the resulting nominal carrier concentration corresponds

[3] Eg. for 2 % Tl doping in PbTe the nominal concentration is 3×10^{20} cm^{-3}, and the measured concentration varies between $5 - 10 \times 10^{19}$ cm^{-3}

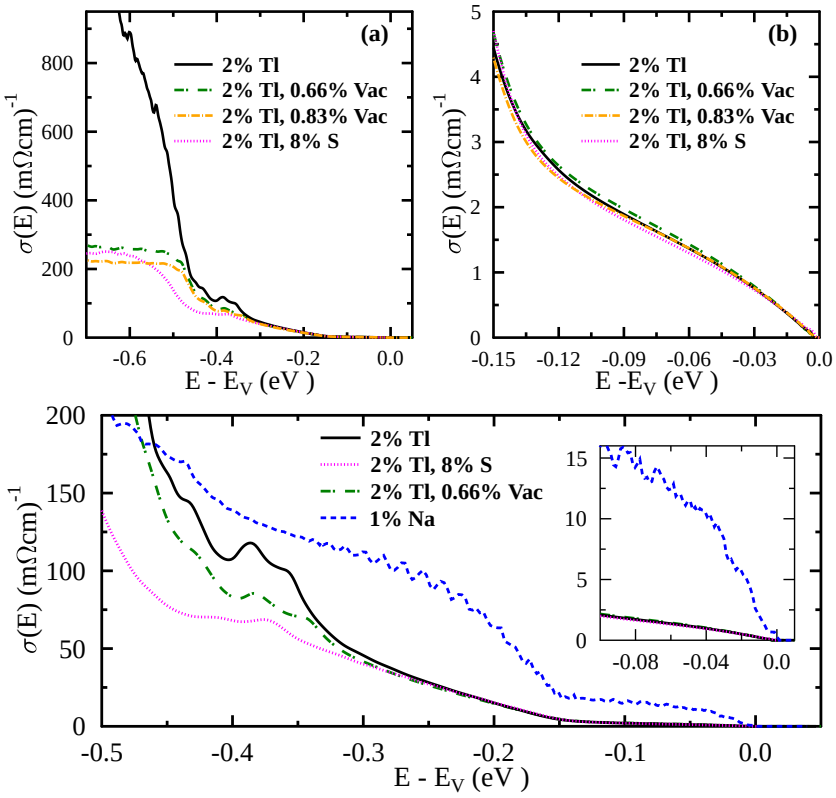

Figure 20: Transport functions of 2% Tl-doped PbTe with Te vacancies or Te/S substitution. Panel (b) shows the zoom of the panel (a) near the VB edge, set as zero of energy. Transport function of 1% Na-doped PbTe compared to 2% Tl-doped PbTe. Inset shows the zoom near the VB edge, set as zero of energy.

to low-temperature measurements using the Hall effect.[4] In the majority of measurements, for 2% of Tl in PbTe, the Hall carrier concentration at helium temperatures was equal to approximately $p = 10^{20}$ cm^{-3}, which requires 0.66% of vacancies on Te, and the majority of my calculations focused on this composition.

To emphasize the contrast between the "classic" and the resonant doping cases, the results for PbTe:Tl are discussed in comparison to PbTe:Na. Comparison of the density of states (Figure 6 in the publication) and spectral functions (Figure below) shows a weak disturbance of the PbTe electron structure by the Na dopant, in contrast to the resonant Tl effect. Strongly blurred PbTe:Tl valence band confirms that the use of Kubo formalism is the only method that allows for accurate consideration of the resonance effect in transport calculations. The exact shape of the spectral functions for single **k**-points was also analyzed and the results clearly showed the non-Lorentzian character of BSF in PbTe:Tl, with the formation of a "shoulder" next to the BSF maximum, in contrast to PbTe:Na (Fig. 8 in the publication). Such a BSF shape allows only a very approximate determination of the electrons' life time, which turned out to be more than an order of magnitude reduced by strong resonant scattering (Figure 9 in the publication).

Transport functions for PbTe with Tl and Na dopings, vacancies on the Te sites, and for one case of the Pb(Te-S) alloy doped with 2% Tl are collected in Fig. 20. The most important features of the computed $\sigma(E)$ functions are:

[4]It is worth noting that Fermi surface anisotropy in PbTe can not be responsible for such large differences in nominal and Hall carrier concentrations, as demonstrated by my (unpublished) calculations of Hall resistance for pure PbTe, analogous to those presented in the work **[H11]**.

- In systems with 2% doped Tl in the region near the edge of the valence band (where the resonant state develops) the conductivity is determined by the presence of resonance, i.e. the additional presence of vacancies or S atoms in the Te position has no effect on $\sigma(E)$, revealing only for deeper states;

- The presence of Tl significantly reduces $\sigma(E)$ in relation to the case of PbTe:Na, which is directly related to shorter life times of electronic states in the presence of resonance.

To refer to the experiment, the determined residual resistivity values $\rho_0 = 1/\sigma(E_F)$ were compared with those available in the literature in Table I in the publication. Satisfactory agreement with the measurements was obtained and, above all, the differences in ρ_0 for PbTe:Tl and Na were correctly reproduced, where the presence of resonance on Tl raises the resistivity about 30 times. This is an independent proof of resonance in PbTe:Tl and its correct description within the framework of KKR-CPA formalism, and gives a hint for future research that residual resistance analysis in samples of good quality (in which scattering on dopants predominates) may indicate the presence or absence of a resonant state. Importantly, the analysis of experimental data shows that at higher temperatures the difference in the mobility of carriers in both materials is no longer that large – electron-phonon scattering causes a drop in life times in PbTe:Na, so that at room temperature the mobility ratio, comparing to Tl, is 2:1. This lower sensitivity of the resonance system to the scattering on phonons causes that, despite strong scattering on the resonant state, it is possible to obtain high values of the power factor PF for elevated temperatures T.

The obtained transport functions $\sigma(E)$ were then used to calculate the thermopowers of the investigated materials, and the results, along with experimental data, are summarized in Fig. 21. First of all, the calculations clearly show that the thermopower in PbTe is increased in the presence of Tl resonant state, in relation to the "regular" Na doping. This result dispels doubts whether the resonant state can actually increase the thermopower in semiconductors, and confirms that resonance on the dopant is the cause of good thermoelectric properties of PbTe:Tl in the range of holes concentration $5-10\times10^{19}$ cm^{-3}. The comparison with the experiment shows that the obtained theoretical results for both systems, PbTe with Tl and Na, are overestimated for concentrations above about 2×10^{19} cm^{-3}. This problem has been discussed in detail in the publication, and is probably related to the too high position of the second maximum of the valence band, which is located at the Σ point of the Brillouin zone, and corresponds to the inaccuracy of exchange-correlation functional. However, this error is a systematic error, present both for the Tl and the Na dopings, therefore it does not affect the conclusion on the relative increase of the thermopower through resonance on Tl.

In the further part of the work I confronted the obtained results with a more qualitative and intuitive explanation of the resonance effect by increasing the effective mass, because such arguments are most often put forward in experimental works. The calculations confirmed that the effective mass for PbTe:Tl is significantly higher than for PbTe:Na, which explains in a simplified way the increase in the thermopower in the system. Qualitative, the resonance works in a way analogous to the increase in band degeneration – by shifting the electronic states from below the Fermi level near the edge of the valence band, it increases the number of states involved in transport phenomena, increasing the material's thermopower. Also, simplified criterion, based on the Mott formula, where $S \propto -d\ln\sigma(E)/dE$, supports the larger thermopower value in PbTe:Tl, against PbTe:Na (see, Fig. 14 in the publication), giving another simplified explanation for the increase in thermopower. On the other hand, the resonance effect should be not compared to the "best thermoelectric" idea (which was done in literature), formulated independently of resonances by Mahan & Sofo [43]. In that idea, the transport function is a Dirac delta function, which is completely different from the $\sigma(E)$ functions, observed in the studied

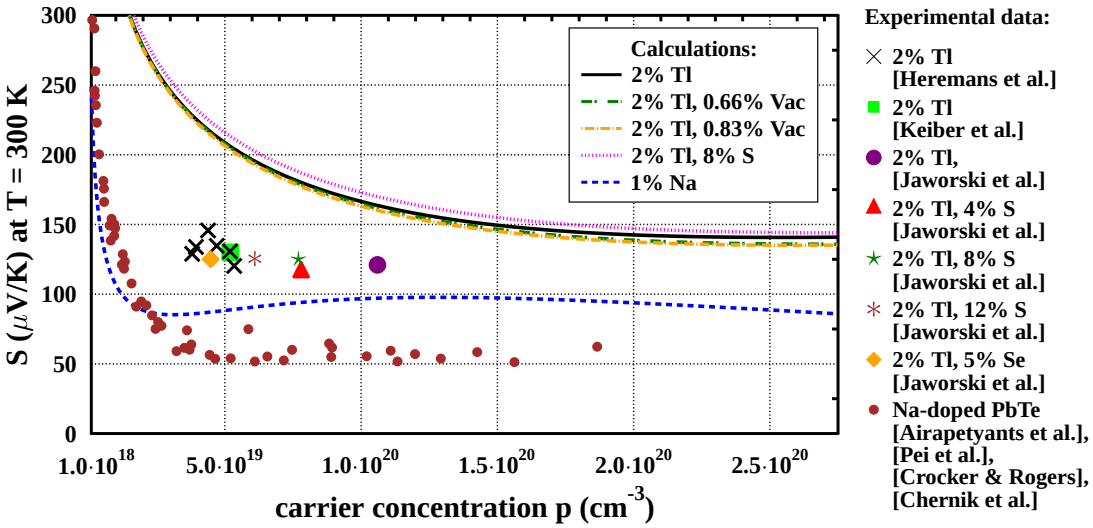

Figure 21: Thermopower at $T = 300$ K as a function of hole concentration (Pisarenko plot) of 2% Tl-doped PbTe containing Te vacancies or Te/S substitution, compared to 1% Na-doped PbTe. Points show experimental results, as described in the legend, from Heremans *et al.* [5], Jaworski *et al.* [37], Keiber *et al.* [38], Pei *et al.* [39], Airapetyants *et al.* [40], Crocker & Rogers [41], Chernik *et al.* [42]. As it is rather impossible to obtain 2% Tl-doped PbTe samples with $p < 10^{19}$ cm^{-3}, this part of the plot does not describe any real material, and is left only for the completeness of the plot.

materials. The last simplified explanation of the increase of thermopower is through the effect of E_F reduction for the given carrier concentration. Calculations have shown, that to reach the holes concentration around 10^{20} cm−3, in PbTe:Na E_F has to be about 100 meV deeper in the valence band, than in PbTe:Tl. Since approximately $S \propto 1/E_F$ [1], lower E_F leads to the higher S.

At the end, it is worth noting the differences between the metallic (Cu-Ni) and semiconducting (PbTe:Tl) resonant system. In PbTe:Tl, conductivity is proportional to the density of states, $\sigma(E) \propto n(E)$, while in constantan we had $\sigma(E) \propto 1/n(E)$ (see figures in the publication). Looking at the basic formula $\sigma = \frac{ne^2\tau}{m^*}$, in the PbTe:Tl case, energy dependence of $\sigma(E)$ is controlled by the change in the number of charge carriers, n, which increases more rapidly while E is going deeper into the valence band than the τ decreases. This results in the proportionality of $\sigma(E)$ and $n(E)$ functions, and shows that the scattering of electrons due to the presence of s-like resonant level in PbTe:Tl is not such a dominant factor, as in the case of RL on Ni in the Cu-Ni alloy. In constantan, s-like carriers are strongly scattered on a $3d$-resonance, thus $\sigma(E)$ drops when E enters the resonant DOS region (Fig. 3 in publication). This explains the difference in sign of thermopowers of constantan, which is negative, and PbTe:Tl, which is positive.

Summary

The series of articles **[H1]**–**[H12]** presents the results of comprehensive research on the issue of formation of resonant states in doped materials, mainly semiconductors, and their influence on the electronic structure and transport properties. The following are the most important results of these works:

1. Showing that resonance states do not necessarily lead to the formation of impurity bands or introduce localized electronic states to the crystal, but by modifying the band structure of the doped compound can shift states from deeper regions below E_F towards the band edge, where they can participate in transport phenomena.

2. Prediction of formation of previously unknown resonant states in tetradymites and the Bi-Sb alloy.

3. Observation and explanation of the new doping mechanism, by creating a deep resonant state, without significant disturbance of the electronic structure of the material at E_F. This mechanism can lead to the acceptor behavior of dopants even with the isovalent substitution of elements.

4. Theoretical confirmation and explanation of the mechanism of increase in thermopower in the semiconductor with resonant dopants, on the example of PbTe:Tl.

The results of my papers contribute to a better understanding of the electronic properties of materials with resonant impurities and can be used to synthesize more efficient thermoelectric materials.

Bibliography

[1] H. J. Goldsmid, *Introduction to Thermoelectricity*. Springer-Verlag Berlin Heidelberg, 2010.

[2] D. Rowe, "Applications of nuclear-powered thermoelectric generators in space," *Applied Energy*, vol. 40, no. 4, pp. 241–271, 1991.

[3] B. Orr, A. Akbarzadeh, M. Mochizuki, and R. Singh, "A review of car waste heat recovery systems utilising thermoelectric generators and heat pipes," *Applied Thermal Engineering*, vol. 101, pp. 490–495, 2016.

[4] Zhao Li-Dong, Lo Shih-Han, Zhang Yongsheng, Sun Hui, Tan Gangjian, Uher Ctirad, Wolverton C., Dravid Vinayak P., and Kanatzidis Mercouri G., "Ultralow thermal conductivity and high thermoelectric figure of merit in SnSe crystals," *Nature*, vol. 508, p. 373, apr 2014.

[5] J. P. Heremans, V. Jovovic, E. S. Toberer, A. Saramat, K. Kurosaki, A. Charoenphakdee, S. Yamanaka, and G. J. Snyder, "Enhancement of thermoelectric efficiency in pbte by distortion of the electronic density of states," *Science*, vol. 321, no. 5888, pp. 554–557, 2008.

[6] B. L. Györffy and G. M. Stocks, "First principles band theory for random metallic alloys," in *Electrons in Disordered Metals and at Metallic Surfaces* (P. Phariseau, B. L. Györffy, and L. Scheire, eds.), NATO ASI Series, Springer-Verlag US, 1979.

[7] J. P. Heremans, B. Wiendlocha, and A. M. Chamoire, "Resonant levels in bulk thermoelectric semiconductors," *Energy Environ. Sci.*, vol. 5, pp. 5510–5530, 2012.

[8] F. J. Blatt, P. A. Schroeder, C. L. Foiles and D. Greig, *Thermoelectric Power of Metals*. Plenum Press, New York, 1976.

[9] A. N. Gerritsen and J. Korringa, "Anomalous resistance of noble metals containing paramagnetic ions," *Phys. Rev.*, vol. 84, pp. 604–605, Nov 1951.

[10] J. Korringa and A. Gerritsen, "The cooperative electron phenomenon in dilute alloys," *Physica*, vol. 19, no. 1, pp. 457 – 507, 1953.

[11] J. Friedel, "On some electrical and magnetic properties of metallic solid solutions," *Canadian Journal of Physics*, vol. 34, no. 12A, pp. 1190–1211, 1956.

[12] J. Callaway and N. H. March, *Density Functional Methods: Theory and Applications*. Solid State Physics, vol. 38, Academic Press, 1984.

[13] S. Kaprzyk and A. Bansil, "Green's function and a generalized Lloyd formula for the density of states in disordered muffin-tin alloys," *Phys. Rev. B*, vol. 42, pp. 7358–7362, Oct 1990.

[14] A. Bansil, S. Kaprzyk, P. E. Mijnarends, and J. Toboła, "Electronic structure and magnetism of $Fe_{3-x}V_xX$ ($X = Si$, Ga, and Al) alloys by the KKR-CPA method," *Phys. Rev. B*, vol. 60, pp. 13396–13412, Nov 1999.

[15] T. Stopa, S. Kaprzyk, and J. Tobola, "Linear aspects of the Korringa-Kohn-Rostoker formalism," *J. Phys.: Cond. Matt.*, vol. 16, no. 28, pp. 4921–4933, 2004.

[16] H. Ebert et al. *The Munich SPR-KKR package, version 6.3.1. and 7.7.1. http://ebert.cup.uni-muenchen.de/SPRKKR*, 2012.

[17] H. Ebert, D. Ködderitzsch, and J. Minár, "Calculating condensed matter properties using the KKR-Green's function method – recent developments and applications," *Reports on Progress in Physics*, vol. 74, p. 096501, Sept. 2011.

[18] P. Blaha, K. Schwarz, G. Madsen, D. Kvasnicka, and J. Luitz, *WIEN2k, An Augmented Plane Wave + Local Orbitals Program for Calculating Crystal Properties (Karlheinz Schwarz, Techn. Universität Wien, Austria).* 2001.

[19] J. D. König, M. D. Nielsen, Y.-B. Gao, M. Winkler, A. Jacquot, H. Böttner, and J. P. Heremans, "Titanium forms a resonant level in the conduction band of pbte," *Phys. Rev. B*, vol. 84, p. 205126, Nov 2011.

[20] H. Ebert, A. Vernes, and J. Banhart, "Relativistic bandstructure of disordered magnetic alloys," *Solid State Communications*, vol. 104, no. 4, pp. 243–247, 1997.

[21] J. S. Faulkner and G. M. Stocks, "Calculating properties with the coherent-potential approximation," *Phys. Rev. B*, vol. 21, pp. 3222–3244, Apr 1980.

[22] B. E. A. Gordon, W. E. Temmerman, and B. L. Gyorffy, "On the fermi surfaces of paramagnetic cu c ni 1-c alloys," *Journal of Physics F: Metal Physics*, vol. 11, no. 4, p. 821, 1981.

[23] W. H. Butler, "Theory of electronic transport in random alloys: Korringa-kohn-rostoker coherent-potential approximation," *Phys. Rev. B*, vol. 31, pp. 3260–3277, Mar 1985.

[24] K. Hoang and S. D. Mahanti, "Electronic structure of Ga-, In-, and Tl-doped PbTe: A supercell study of the impurity bands," *Phys. Rev. B*, vol. 78, p. 085111, Aug. 2008.

[25] Y. Imai, Y. Mori, S. Nakamura, and K.-i. Takarabe, "Energetic consideration of the conduction type of Mg2Si doped with Cu, Ag, or Au using first-principle calculations," *Journal of Alloys and Compounds*, vol. 549, pp. 175–178, 2013.

[26] A. Prytuliak, E. Godlewska, K. Mars, and D. Berthebaud, "Synchrotron Study of Ag-Doped Mg2Si: Correlation Between Properties and Structure," *Journal of Electronic Materials*, vol. 43, pp. 3746–3752, Oct 2014.

[27] C. M. Jaworski, V. Kulbachinskii, and J. P. Heremans, "Resonant level formed by tin in bi_2te_3 and the enhancement of room-temperature thermoelectric power," *Phys. Rev. B*, vol. 80, p. 233201, Dec 2009.

[28] J. P. Heremans and B. Wiendlocha, "Tetradymites: Bi_2Te_3-Related Materials," in *Materials Aspect of Thermoelectricity* (C. Uher, ed.), Taylor and Francis, Boca Raton, FL, USA, 2017.

[29] M. Fuccillo, S. Jia, M. Charles, and R. Cava, "Thermoelectric Properties of Bi_2Te_2Se Compensated by Native Defects and Sn Doping," *Journal of Electronic Materials*, vol. 42, no. 6, pp. 1246–1253, 2013.

[30] B. Wiendlocha, H. Jin, J. Tobola, S. Kaprzyk, and J. P. Heremans, "Search for resonant impurities in bismuth and bismuth antimony alloys—First principles study," *The 30th International Conference on Thermoelectrics, 2011. July 17–21, Traverse City, MI (USA).*

[31] J. P. Heremans, H. Jin, and B. Wiendlocha, "Potassium is a resonant level in $Bi_{1-x}Sb_x$ alloys," *APS March Meeting, 2012. February 27–March 2, Boston, MA. (USA).*

[32] H. Jin, B. Wiendlocha, C. Orovets, and J. P. Heremans, "Thermoelectric properties of alkali-doped Bismuth-Antimony alloys and discovery of potassium as a resonant impurity," *The 31th International Conference on Thermoelectrics, 2012. July 9–12, Aalborg, Denmark.*

[33] R. Kubo, "Statistical-mechanical theory of irreversible processes. i. general theory and simple applications to magnetic and conduction problems," *Journal of the Physical Society of Japan*, vol. 12, no. 6, pp. 570–586, 1957.

[34] D. A. Greenwood, "The boltzmann equation in the theory of electrical conduction in metals," *Proceedings of the Physical Society*, vol. 71, no. 4, p. 585, 1958.

[35] C. Y. Ho, M. W. Ackerman, K. Y. Wu, S. G. Oh, and T. N. Havill, "Thermal conductivity of ten selected binary alloy systems," *Journal of Physical and Chemical Reference Data*, vol. 7, no. 3, pp. 959–1178, 1978.

[36] A. Vernes, H. Ebert, and J. Banhart, "Electronic conductivity in $\mathrm{ni}_x\mathrm{cr}_{1-x}$ and $\mathrm{ni}_x\mathrm{cu}_{1-x}$ fcc alloy systems," *Phys. Rev. B*, vol. 68, p. 134404, Oct 2003.

[37] C. M. Jaworski, B. Wiendlocha, V. Jovovic, and J. P. Heremans, "Combining alloy scattering of phonons and resonant electronic levels to reach a high thermoelectric figure of merit in pbtese and pbtes alloys," *Energy Environ. Sci.*, vol. 4, pp. 4155–4162, 2011.

[38] T. Keiber, F. Bridges, B. C. Sales, and H. Wang, "Complex role for thallium in PbTe:Tl from local probe studies," *Phys. Rev. B*, vol. 87, p. 144104, Apr 2013.

[39] Y. Pei, A. LaLonde, S. Iwanaga, and G. J. Snyder, "High thermoelectric figure of merit in heavy hole dominated pbte," *Energy Environ. Sci.*, vol. 4, pp. 2085–2089, 2011.

[40] S. V. Airapetyants, M. N. Vinograd, I. N. Dubrovsk, N. V. Kolomoet and I. M. Rudnik, "Structure of the valence band of heavily doped lead telluride," *Soviet Physics Solid State*, vol. 8, pp. 1069–1072, 1966.

[41] A. J. Crocker and L. M. Rogers, "Interpretation of the hall coefficient, electrical resistivity and seebeck coefficient of p-type lead telluride," *British Journal of Applied Physics*, vol. 18, no. 5, p. 563, 1967.

[42] I. A. Chernik, V. I. Kaidanov, M. I. Vinogradova and N. V. Kolomoets, "Investigation of the valence band of lead telluride using transport phenomena," *Sov. Phys. Semiconduct.*, vol. 2, p. 645–651, 1968.

[43] G. D. Mahan and J. O. Sofo, "The best thermoelectric," *Proceedings of the National Academy of Sciences*, vol. 93, no. 15, pp. 7436–7439, 1996.

5. Description of other scientific achievements

My other research interests can be grouped into three categories: (i) studies of thermoelectric materials (without resonant impurities), (ii) studies of superconductors, (iii) studies of magnetic and magnetocaloric materials. Below I will briefly describe some of the most important results, from the point of view of my theoretical works and contribution.

5.1. Papers on the thermoelectric materials

[P1] Joseph P. Heremans and Bartlomiej Wiendlocha, "Tetradymites: Bi_2Te_3-Related Materials". Rozdział w monografii "Materials Aspect of Thermoelectricity", ed. Ctirad Uher, CRC Press, Boca Raton, FL (USA), 2017, strony 39-94.

[P2] Jean-Baptiste Vaney, Gaelle Delaizir, Bartlomiej Wiendlocha, Janusz Tobola, Eric Alleno, Andrea Piarristeguy, Antonio Pereira Gonçalves, Christine Gendarme, Bernard Malaman, Anne Dauscher, Christophe Candolfi, and Bertrand Lenoir, "Effect of Isovalent Substitution on the Electronic Structure and Thermoelectric Properties of the Solid Solution α-$As_2Te_{3-x}Se_x$ ($0 \leqslant x \leqslant 1.5$)", Inorganic Chemistry **56**, 2248 (2017).

[P3] K. Kutorasinski, B. Wiendlocha, S. Kaprzyk, and J. Tobola, "Electronic structure and thermoelectric properties of n- and p-type SnSe from first-principles calculations", Physical Review B **91**, 205201 (2015).

[P4] K. Kutorasinski, B. Wiendlocha, J. Tobola, and S. Kaprzyk, "Importance of relativistic effects in electronic structure and thermopower calculations for Mg_2Si, Mg_2Ge, and Mg_2Sn", Phys. Rev. B **89**, 115205 (2014).

[P5] J. Bourgeois, J. Tobola, B. Wiendlocha, L. Chaput, P. Zwolenski, D. Berthebaud, F. Gascoin, Q. Recour, H. Scherrer, "Study of electron, phonon and crystal stability versus thermoelectric properties in Mg_2X (X = Si, Sn) compounds and their alloys", Functional Materials Letters **6**, 1340005 (2013)

[P6] C. Candolfi, B. Lenoir, A. Dauscher, E. Guilmeau, J. Hejtmanek, J. Toboła, B. Wiendlocha, S. Kaprzyk, "Transport properties of the Mo_3Sb_7 compound", Physical Reviev B **79**, 035114 (2009).

In addition to thermoelectric systems containing resonant dopants, I was also working on non-doped or doped with "regular" impurities thermoelectric materials. My work focused on the electronic structure of materials and its relationship to electronic transport properties. The most important achievements of the above mentioned works include: [P1] Systematic analysis of the electronic structure, Fermi surface, effective mass and thermopowers for the tetradymites: Bi_2Te_3, Bi_2Se_3 and Sb_2Te_3. Explanation of the reason for the observed in literature overestimation of the theoretical Seebeck coefficient of p-type Bi_2Se_3 (wrong position of the second maximum of the valence band).

[P3] Investigation of anisotropic transport properties of SnSe semiconductor with a record high zT, taking into account changes in the crystal structure as a function of temperature. Prediction of very good thermoelectric properties of n-type material.

[P4] Examination of the effect of the spin-orbit coupling on the electronic structure, effective mass and thermopower of Mg_2Si, Mg_2Ge, and Mg_2Sn. Demonstration (previously unnoticed) of the huge impact of spin-orbit coupling on the thermopower of Mg_2Sn.

5.2. Papers on superconductors

[P7] Judyta Strychalska-Nowak, Bartłomiej Wiendlocha, Katarzyna Hołowacz, Paula Reczek, Mateusz Podgórski, Michał J Winiarski and Tomasz Klimczuk, "Fermi-liquid behavior of binary intermetallic compounds Y3M (M = Co, Ni, Rh, Pd, Ir, Pt)",Mater. Res. Express **4**, 066501 (2017)

[P8] B. Wiendlocha, R. Szczęśniak, A. P. Durajski, M. Muras, "Pressure effects on the unconventional superconductivity of noncentrosymmetric $LaNiC_2$", Physycial Review B **94**, 134517 (2016).

[P9] J. Strychalska, M. Roman, Z. Sobczak, B. Wiendlocha, M.J. Winiarski, F. Ronning, T. Klimczuk,"Physical properties and electronic structure of La_3Co and La_3Ni intermetallic superconductors", Physica C **528**, 73 (2016).

[P10] M. J. Winiarski, B. Wiendlocha, S. Gołąb, S. K. Kushwaha, P. Wiśniewski, D. Kaczorowski, J. D. Thompson, R. J. Cava and T. Klimczuk, "Superconductivity in $CaBi_2$", Physical Chemistry Chemical Physics **18**, 21737 (2016).

[P11] M. J. Winiarski, B. Wiendlocha, M. Sternik, P. Wiśniewski, J. R. O'Brien, D. Kaczorowski, and T. Klimczuk, "Rattling-enhanced superconductivity in MV_2Al_{20} (M = Sc,Lu,Y) intermetallic cage compounds", Phys. Rev. B **93**, 134507 (2016)

[P12] K. Jasiewicz, B. Wiendlocha, P. Korbeń, S. Kaprzyk and J. Tobola, "Superconductivity of $Ta_{34}Nb_{33}Hf_8Zr_{14}Ti_{11}$ high entropy alloy from first principles calculations", Physica Status Solidi Rapid Research Letters **10**, 415 (2016)

[P13] B. Wiendlocha, M. J. Winiarski, M. Muras, C. Zvoriste-Walters, J.-C. Griveau, S. Heathman, M. Gazda, and T. Klimczuk, "Pressure effects on the superconductivity of the $HfPd_2Al$ Heusler compound: Experimental and theoretical study", Phys. Rev. B **91**, 024509 (2015).

[P14] Bartlomiej Wiendlocha, Malgorzata Sternik, "Effect of the tetragonal distortion on the electronic structure, phonons and superconductivity in the Mo_3Sb_7 superconductor" Intermetallics **53**, 150 (2014).

[P15] B. Wiendlocha, J. Tobola, S. Kaprzyk, and A. Kolodziejczyk, "Electronic structure, magnetism, and spin fluctuations in the superconducting weak ferromagnet Y_4Co_3", Phys. Rev. B **83**, 094408 (2011).

[P16] B. Wiendlocha, J. Toboła, M. Sternik, S. Kaprzyk, K. Parliński, A. M. Oleś, "Superconductivity of Mo_3Sb_7 from first pronciples", Physical Reviev B **78**, 060507(R) (2008).

[P17] B. Wiendlocha, J. Toboła, S. Kaprzyk, D. Fruchart, "Electronic structure, superconductivity and magnetism study of Cr_3GaN and Cr_3RhN" Journal of Alloys and Compounds **422**, 289 (2007).

[P18] A. Kołodziejczyk, B. Wiendlocha, R. Zalecki, J. Toboła, S. Kaprzyk, "Superconductivity, Weak Itinerant Ferromagnetism and Electronic Band Structure of Y_9Co_7", Acta Physica Polonica A **111**, 513 (2007).

[P19] B. Wiendlocha, J. Toboła, S. Kaprzyk, "Electronic structure of the noncentrosymmetric superconductor $Mg_{10}Ir_{19}B_{16}$" http://arxiv.org/abs/0704.1295

[P20] B. Wiendlocha, J. Toboła, S. Kaprzyk, "Search for Sc_3XB (X = Tl, In, Ga, Al) perovskites superconductors and proximity of weak ferromagnetism", Physical Reviev B **73**, 134522 (2006).

[P21] B. Wiendlocha, J. Toboła, S. Kaprzyk, D. Fruchart, J. Marcus, "Competition of ferromagnetism and superconductivity in Sc_3InB", Physica Status Solidi B, **243**, 351 (2006).

In my works on superconductivity, I studied the electronic structure, dynamic properties and electron-phonon interaction in classical superconductors, i.e. those in which electron-phonon coupling is responsible for superconductivity. In most of the works I used the so-called *rigid muffin tin approximation* (RMTA), in which the electron and phonon contributions are separated, and the electron-phonon coupling constant is calculated on the basis of independent electronic structure and phonon calculations. This allows to study the influence of doping and defects on superconductivity, and allows to study disordered materials as well as very complex structures. I also studied the influence of spin fluctuations on superconductivity. The most interesting results (chronologically from the oldest works) include: [P20] – [P21] Prediction of superconductivity in Sc_3InB and related Sc_3XB structures and the transition from superconductivity to weak ferromagnetism as a function of concentration of boron atoms. The results were partially positively verified experimentally and the decisive effect of the concentration of boron atoms on the value of T_c was obtained.

[P15], [P18] Investigation of the electronic structure and unique, quasi-one-dimensional magnetism of the superconductor Y_4Co_3 / Y_9Co_7, where magnetic moments are located only on the edges of a complex unit cell. The plots of magnetization density distribution from this work were highlighted by the presentation in the rubric it Kaleidoscope on the main page of Physical Review B.

[P14], [P16] We showed that the superconductivity of the Mo_3Sb_7 compound originates from the electron-phonon interaction, which was then the subject of debate in literature, and investigated the influence of spin fluctuations and structural distortion on the superconductivity of this compound.

[P12] Investigation of the electronic structure and determination of the electron-phonon coupling constant of the first superconducting high entropy alloy $Ta_{34}Nb_{33}Hf_8Zr_{14}Ti_{11}$. Results showed that the superconductivity has electron-phonon origin, however in the material there may be enhanced depairing effects, because experimental T_c is significantly lowered.

[P11] The theoretical and experimental investigation of the superconducting properties, electronic structure and dynamic properties of a series of compounds with cage structure MV_2Al_{20} allowed to find that the vibrations of M atoms determine the critical temperature in this series of compounds. In particular, when there is a so-called *rattling* effect – the vibrations of the M atom become anharmonic, low-frequency and separated from other phonon modes – the critical temperature and electron-phonon coupling constant increases, which is best illustrated by the case of ScV_2Al_{20}.

[P10] Examination of the quasi-two-dimensional electronic structure of the new $CaBi_2$ superconductor and of a very strong influence of the spin-orbit coupling on material's properties.

[P8] Calculations of the full electron-phonon coupling function (the so-called Eliashberg function) allowed us to closely examine the evolution of electron-phonon coupling and superconductivity as a function of pressure for unconventional, noncentrosymmetric $LaNiC_2$ superconductor. The calculations have shown that experimentally observed increase in T_c in the lower external pressure regions can be explained by the electron-phonon superconducting mechanism. More interestingly, the disappearance of superconductivity, experimentally observed above 7 GPa, must be associated with the emergence of a new electron phase in the material, because from the point of view of electron-phonon interactions, T_c should continue to grow monotonically.

5.3. Papers on magnetic and magnetocalloric materials

[P22] Bartlomiej Wiendlocha, SunPhil Kim, Yeseul Lee, Bin He, Gloria Lehr, Mercouri G. Kanatzidis, Donald T. Morelli and Joseph P. Heremans, "Eu^{2+} – Eu^{3+} valence transition in double, Eu-, and Na-doped PbSe from transport, magnetic, and electronic structure studies", Physical Chemistry Chemical Physics **19**, 9606 (2017).

[P23] J. Łażewski, P. Piekarz, J. Toboła, B. Wiendlocha, P. T. Jochym, M. Sternik, and K. Parlinski, "Phonon Mechanism of the Magnetostructural Phase Transition in MnAs", Phys. Rev. Lett. **104**, 147205 (2010).

[P24] B. Wiendlocha, J. Toboła, S. Kaprzyk, R. Zach, E. K. Hlil, D. Fruchart, "Magnetocaloric properties of $Fe_{2-x}T_xP$ (T = Ru and Rh) from electronic structure calculations and magnetisation measurements", Journal of Physics D: Applied Physycs **41**, 205007 (2008).

[P25] J. Toboła, B. Wiendlocha, S. Kaprzyk, R. Zach, E. K. Hlil, D. Fruchart, "Electronic structure calculations of ferromagnetic and paramagnetic state in magnetocalloric materials $Mn_{1-x}T_xAs$ and $Fe_{2-x}T_xP$". Proceedings of the 2nd International Conference of the IIR on Magnetic Refrigeration at Room Temperature, 11-13 april 2007, Portoroz, Slovenia. pp. 119-126.

In this point, I would like to mention the results of two works, i.e. [P22] and [P24]. In paper [P22] we investigated the electronic, transport and magnetic properties of the doubly-doped PbSe semiconductor, and the magnetic properties of the system had a key role in understanding the phenomena observed in the material. PbSe is one of the classic semiconductor materials that has been studied for decades in optoelectronic and thermoelectric applications. In particular, PbSe doped with Eu is used for the construction of infrared detectors and lasers. Eu ions, substituted for Pb, exhibit a divalent electron configuration Eu^{2+}, with a half-filled 4f shell (configuration $4f^7$). Eu is therefore a neutral dopant relative to Pb^{2+}, and ions Eu^{2+} have a large, localized magnetic moment $7\mu_B$ of the $4f^7$ shell. In the course of experimental and theoretical research described in this work, we discovered that under the influence of additional Na doping, in PbSe:Eu in a controlled way one can initiate a change in the valence of Eu, from Eu^{2+} ($4f^7$) to Eu^{3+} ($4f^6$), and create a mixed-valence state. This is manifested by spectacular changes in physical properties, i.e. carrier concentration (Eu^{3+} becomes a donor) or magnetisation (Eu^{3+} is non-magnetic) changes by orders of magnitude. The calculations of the electronic structure showed that the additional doping with Na leads to a lowering of the Fermi level close to the density of states peak of Eu^{2+} ions, which induces instability in the system and triggers the transition to a state with mixed Eu valence. This is the first example of controllable change in the valence, by introducing a small amount of additional dopant atoms to the material.

In the paper [P24] detailed calculations of the electronic structure, magnetic properties as well as electronic and magnetic entropy were done for materials based on ferromagnetic Fe_2P, in a ferromagnetic and paramagnetic state, simulated using CPA by disorder of magnetic moments. The aim of the work was to understand and describe the magnetocaloric properties of the system, which are mainly due to the change of magnetic entropy during the phase transition to the paramagnetic state. With the help of numerical calculations and the mean field model, this was done in a very good agreement with the experimental results, which showed a correct understanding of the magnetocaloric effect in these materials. This work was mostly done during my two-month stay at the Institut Néel, CNRS Grenoble in France (french government scholarship) where I also participated in the experimental part of the work.

5.4. Other publications

In addition to scientific publishing, I wrote several articles on the history and activities of the Academic Underwater Club KRAB AGH, with which I am connected for over 15 years (they appeared in national diving magazines, i.e. Underwater World, Great Blue, Diving). In addition, I am the author of the chapter "Physics of Diving" in the textbook "Diving" by Łukasz Mrowiec, published by the Scriptum publishing house from Krakow in 2007.

5.5. Bibliometric data of all the publications

Total number of publications: 37, in the Web of Science database: 33
Number of citations: 694, without self-citations: 596.
Index H: 12

Bartłomiej Wiendlocha